Synthesis of 5-Metalla-spiro[4.5]heterodecenes by [1,4]-Cycloaddition Reaction of Group 13 Diyls with 1,2 Diketones

*Hanns M. Weinert,[1] Christoph Wölper,[1] and Stephan Schulz[1,2,]**

[1] Institute of Inorganic Chemistry, University of Duisburg-Essen, Universitätsstr.5–7, 45141 Essen (Germany)
[2] Center for Nanointegration Duisburg-Essen (CENIDE)University of Duisburg-Essen, Carl-Benz-Straße 199, 47057 Duisburg (Germany)
* Correspondence author: stephan.schulz@uni-due.de

Content

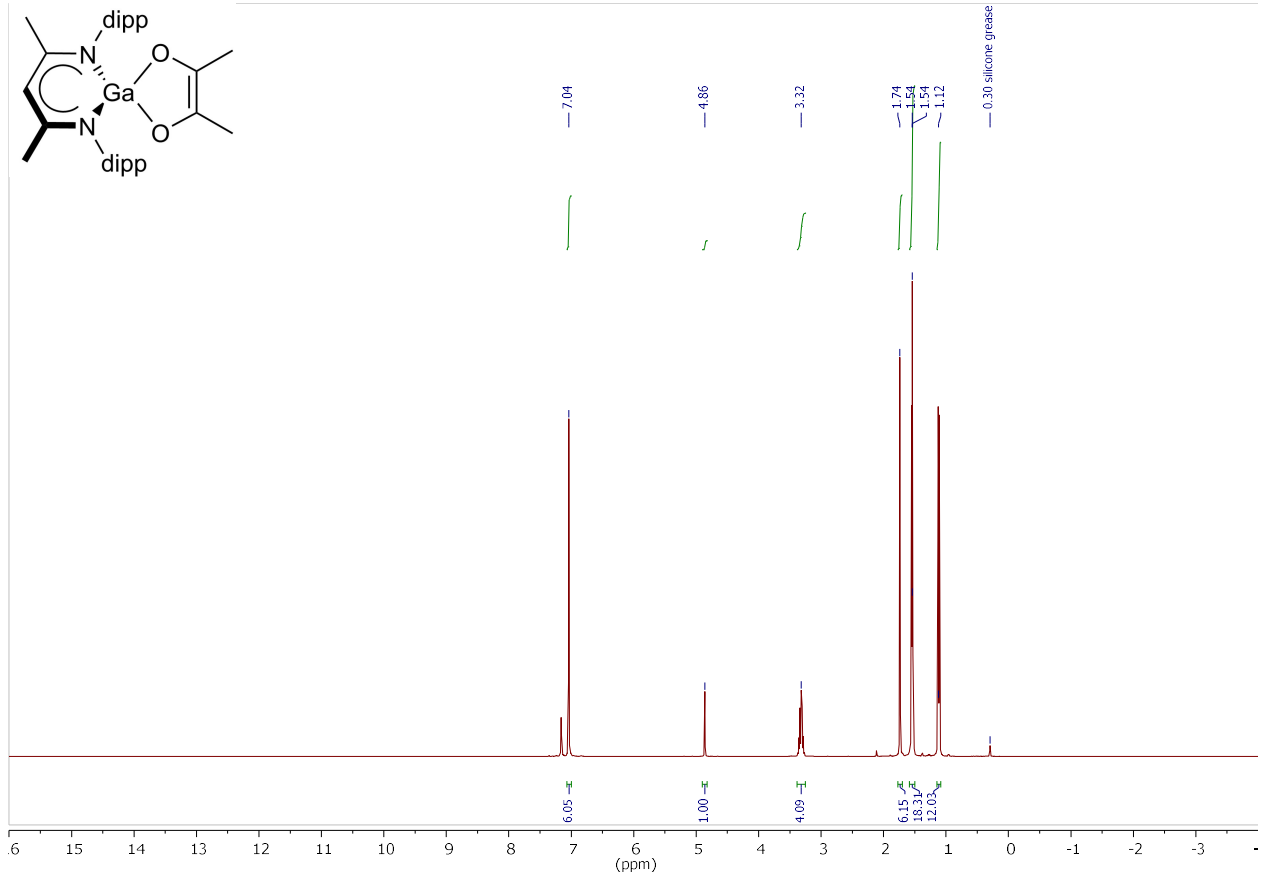

Fig. S1. ^{1}H NMR spectrum (400 MHz, C_6D_6, 25 °C) of LGa($C_4H_6O_2$) (**1**).

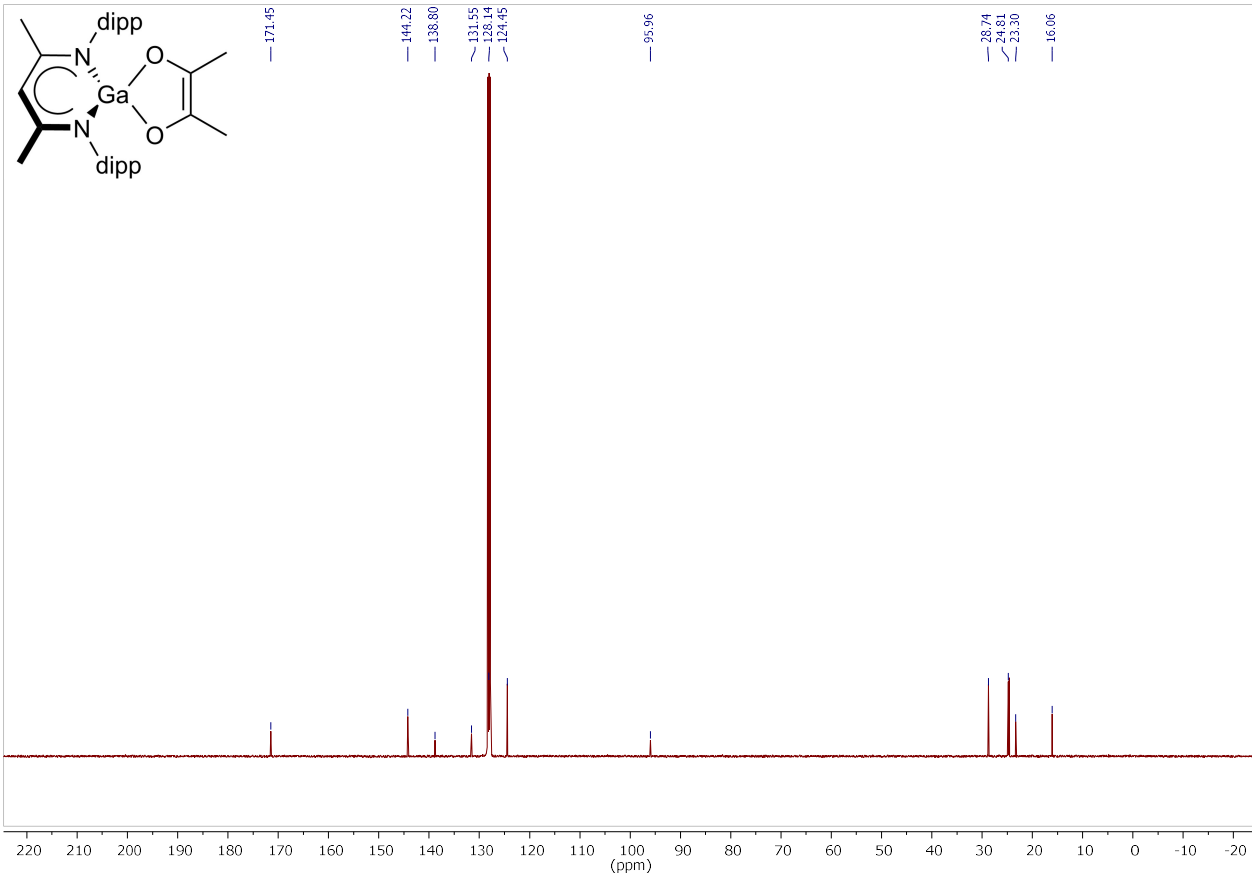

Fig. S2. ^{13}C NMR spectrum (100.6 MHz, C_6D_6, 25 °C) of LGa($C_4H_6O_2$) (**1**).

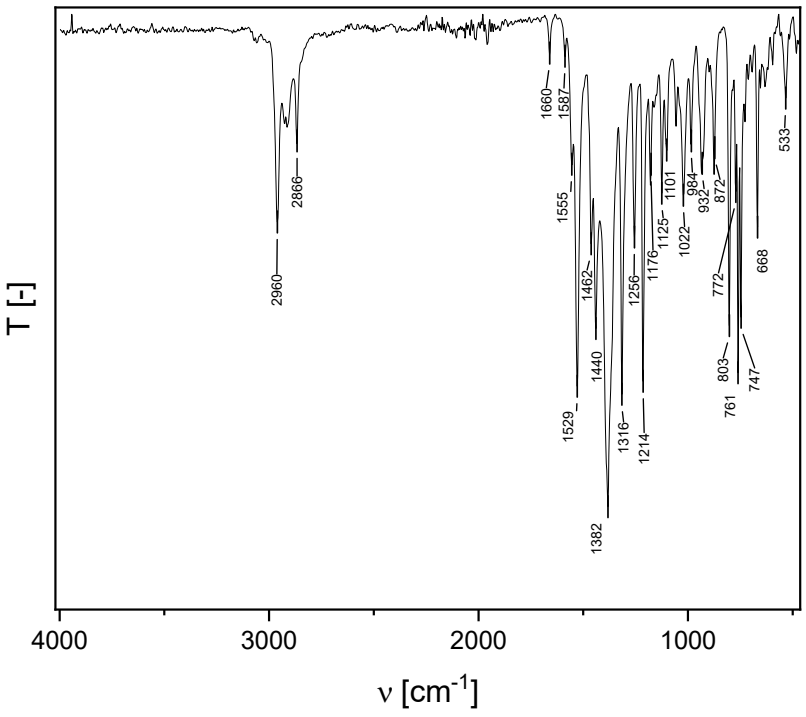

Fig. S3. ATR-IR spectrum of $LGa(C_4H_6O_2)$ (**1**).

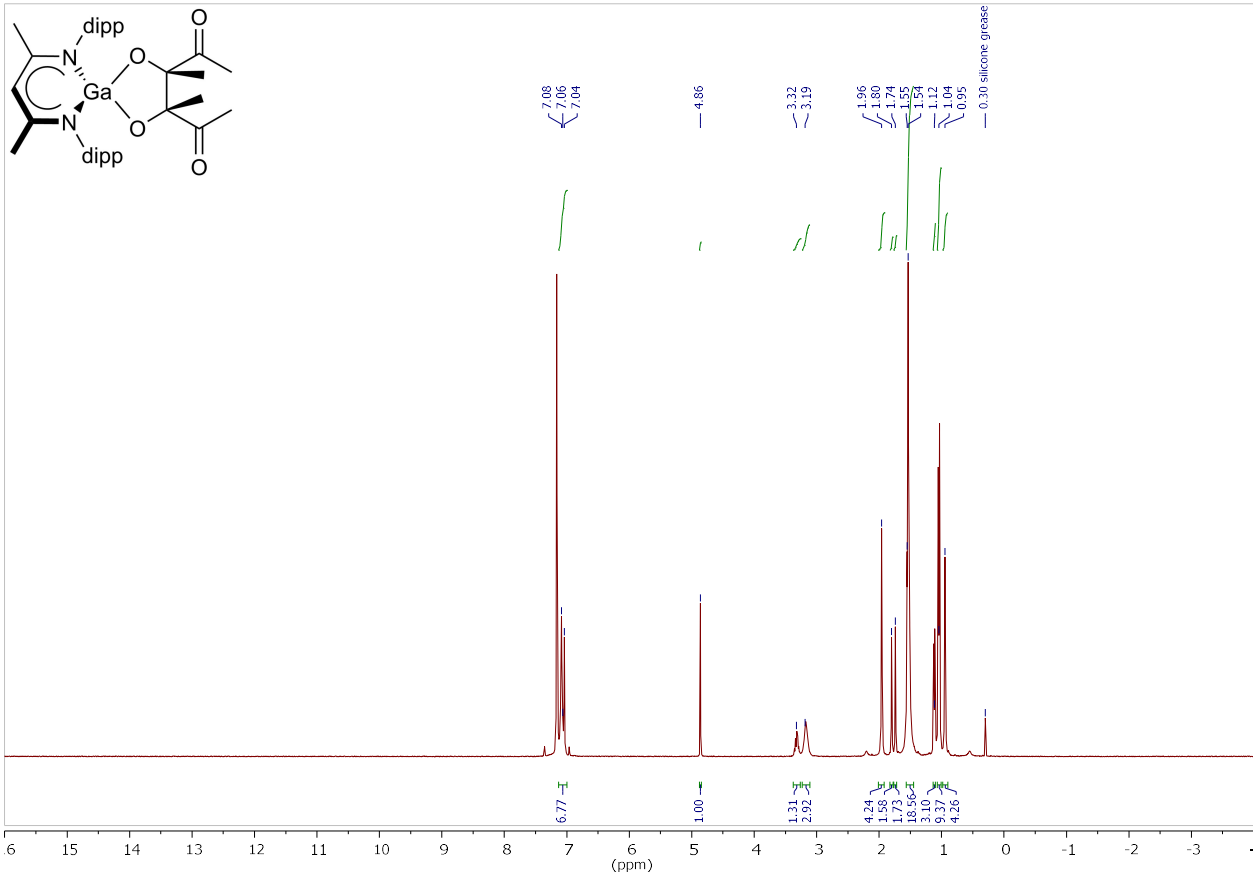

Fig. S4. ^{1}H NMR spectrum (400 MHz, C_6D_6, 25 °C) of $LGa(C_8H_{12}O_{14})$ (**2**).

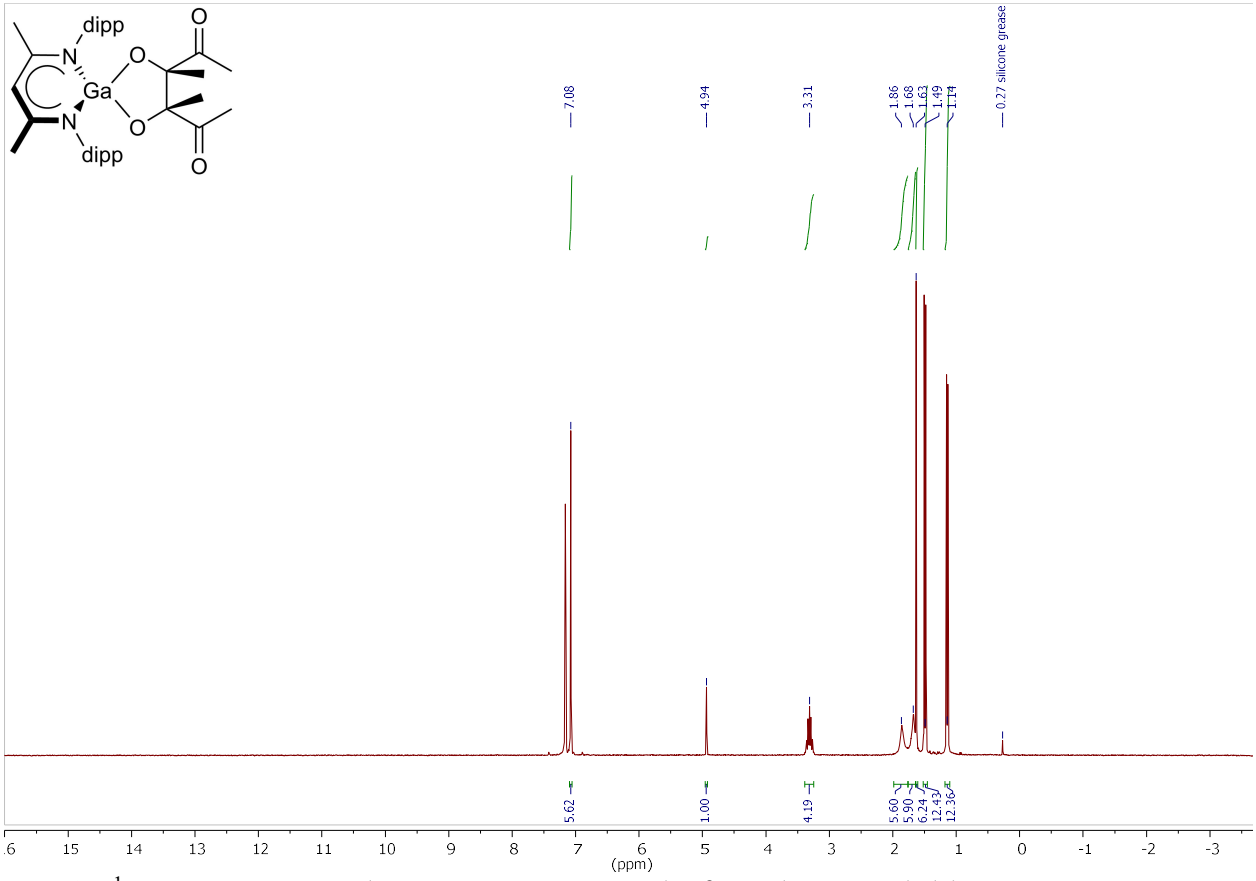

Fig. S5. ^{1}H NMR spectrum (300 MHz, C_6D_6, 80 °C) of LGa($C_8H_{12}O_{14}$) (**2**).

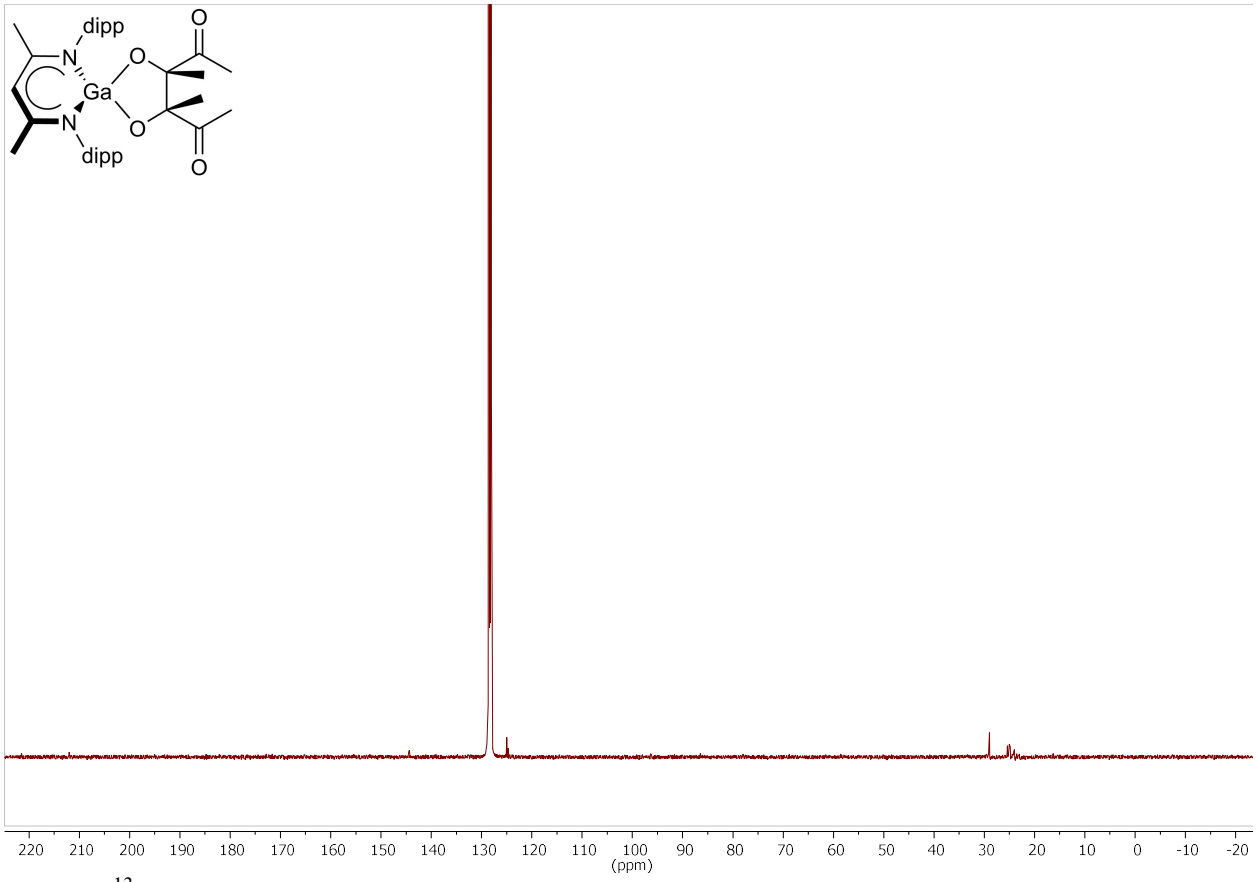

Fig. S6. ^{13}C NMR spectrum (100.6 MHz, C_6D_6, 25 °C) of LGa($C_8H_{12}O_4$) (**2**).

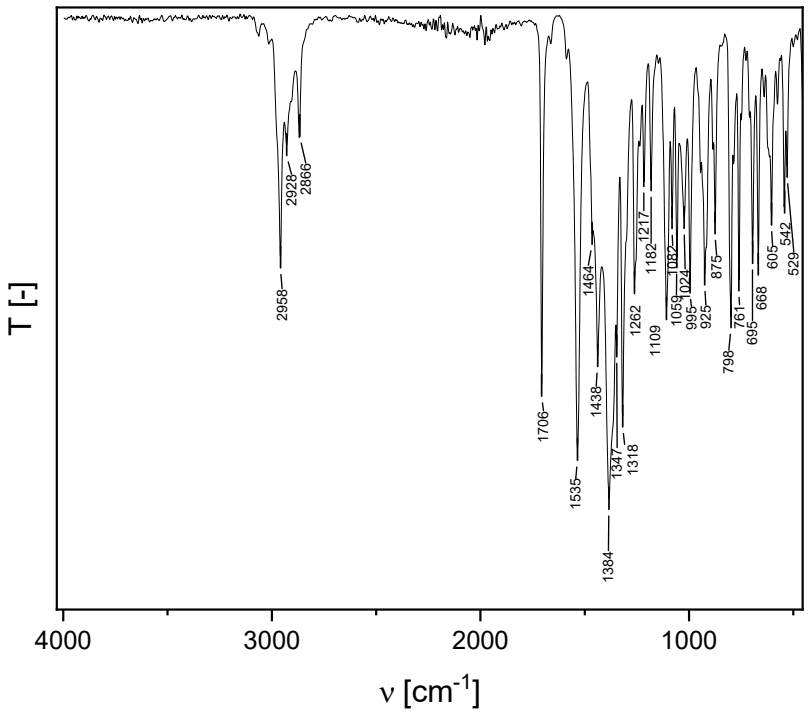

Fig. S7. ATR-IR spectrum of $LGa(C_8H_{12}O_{14})$ (**2**).

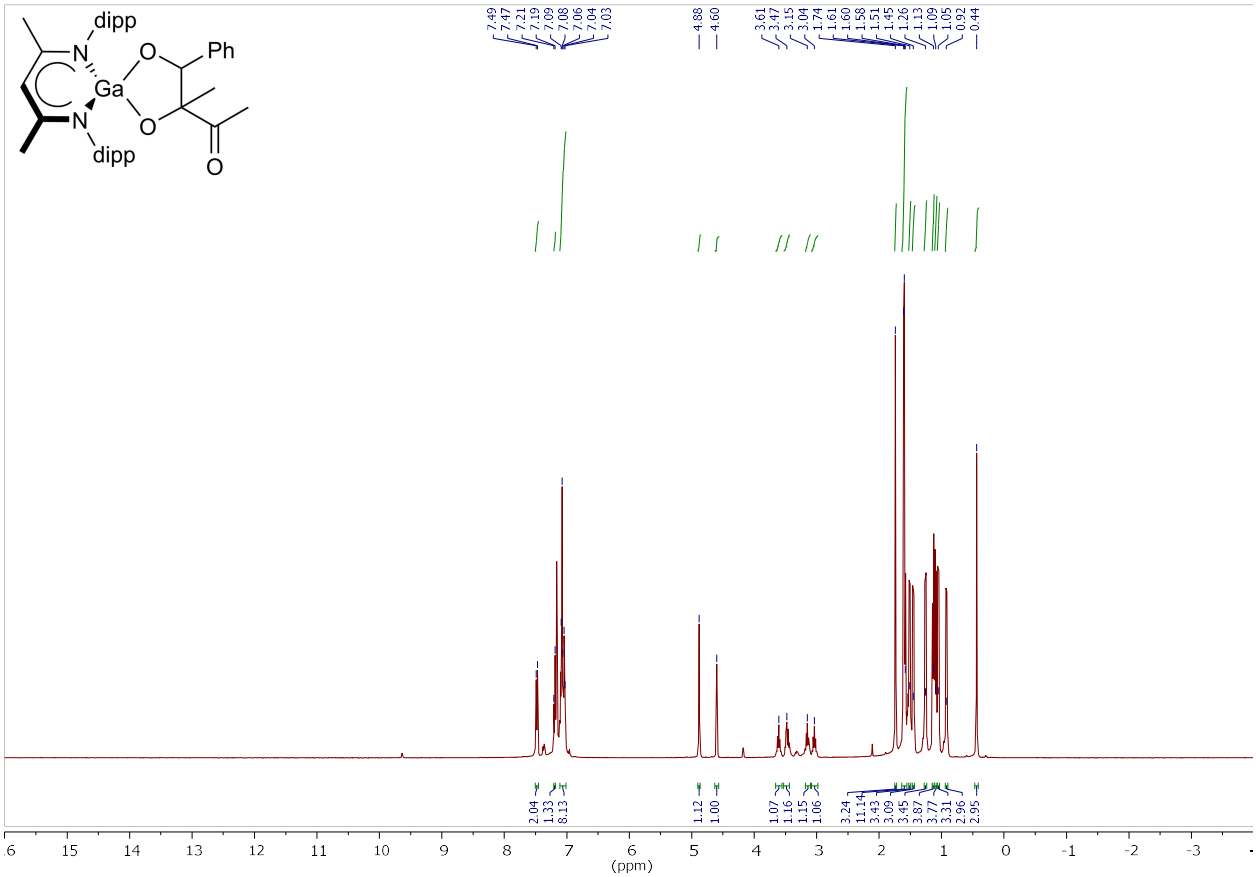

Fig. S8. ^1H NMR spectrum (400 MHz, C_6D_6, 25 °C) of $LGa(C_{11}H_{12}O_3)$ (**3**).

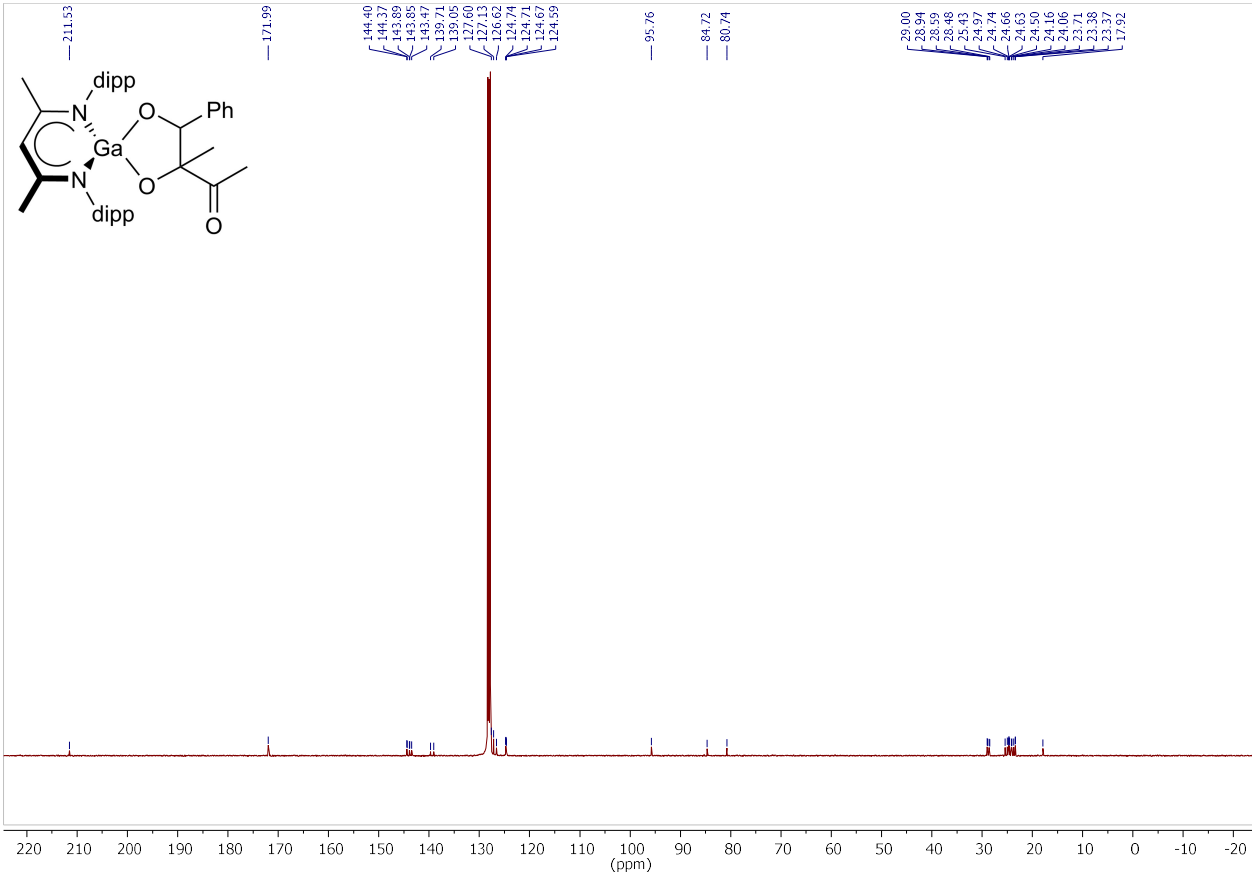

Fig. S9. ^{13}C NMR spectrum (100.6 MHz, C_6D_6, 25 °C) of LGa($C_{11}H_{12}O_3$) (**3**).

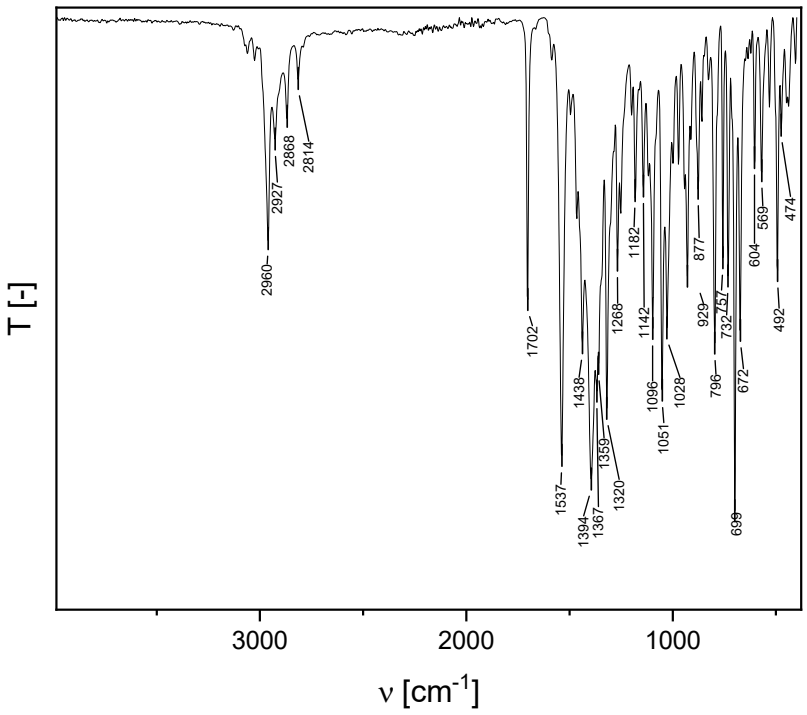

Fig. S10. ATR-IR spectrum of LGa($C_{11}H_{12}O_3$) (**3**).

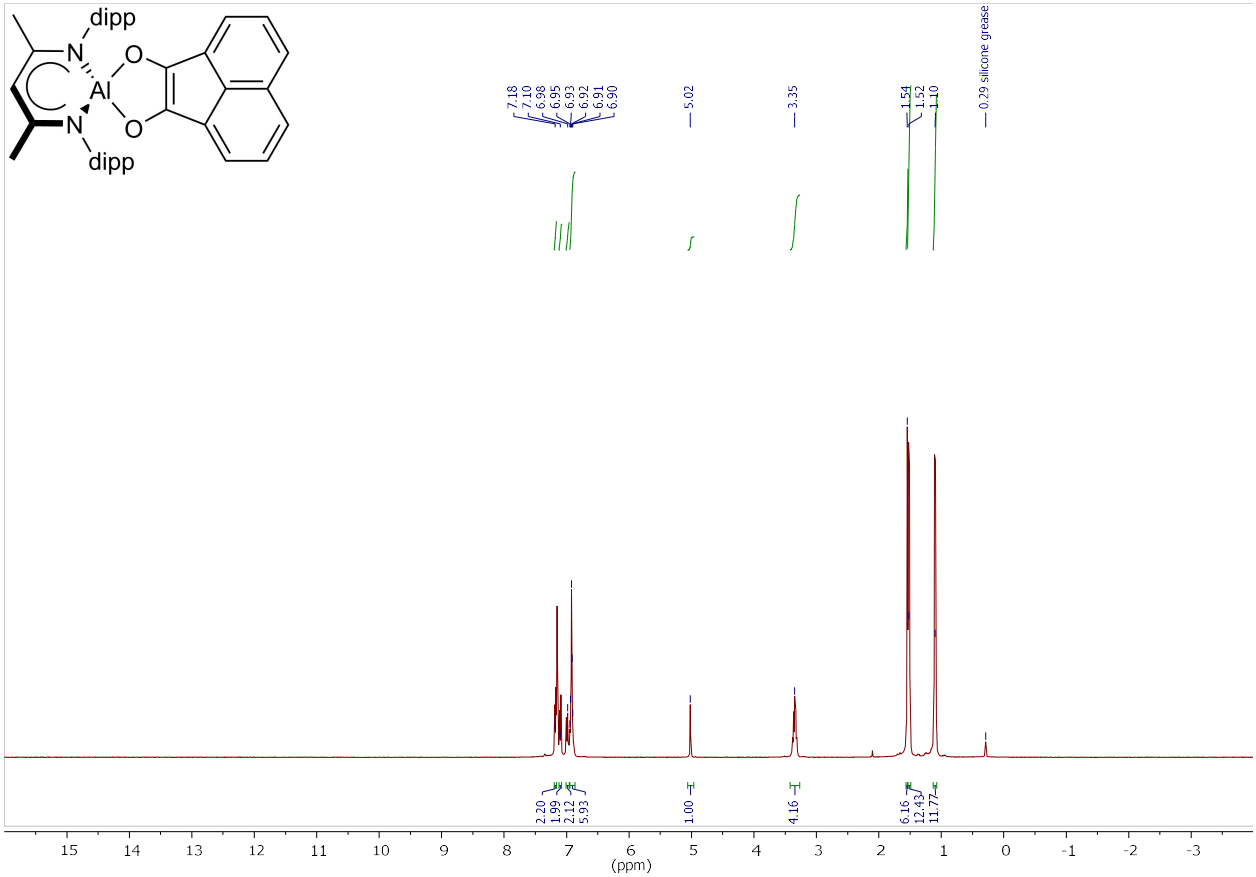

Fig. S11. ^{1}H NMR spectrum (400 MHz, C_6D_6, 25 °C) of LAl($C_{12}H_6O_2$) (**4**).

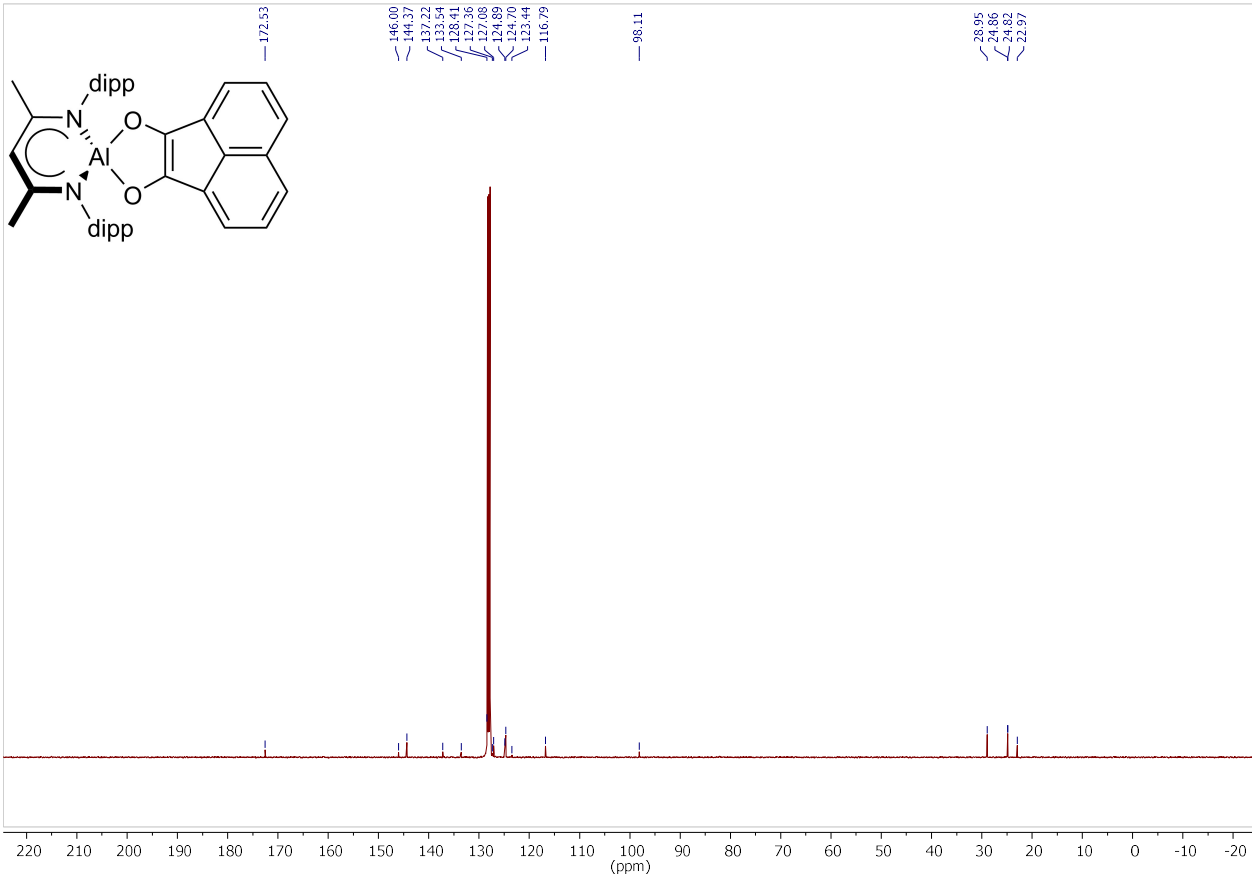

Fig. S12. ^{13}C NMR spectrum (100.6 MHz, C_6D_6, 25 °C) of LAl($C_{12}H_6O_2$) (**4**).

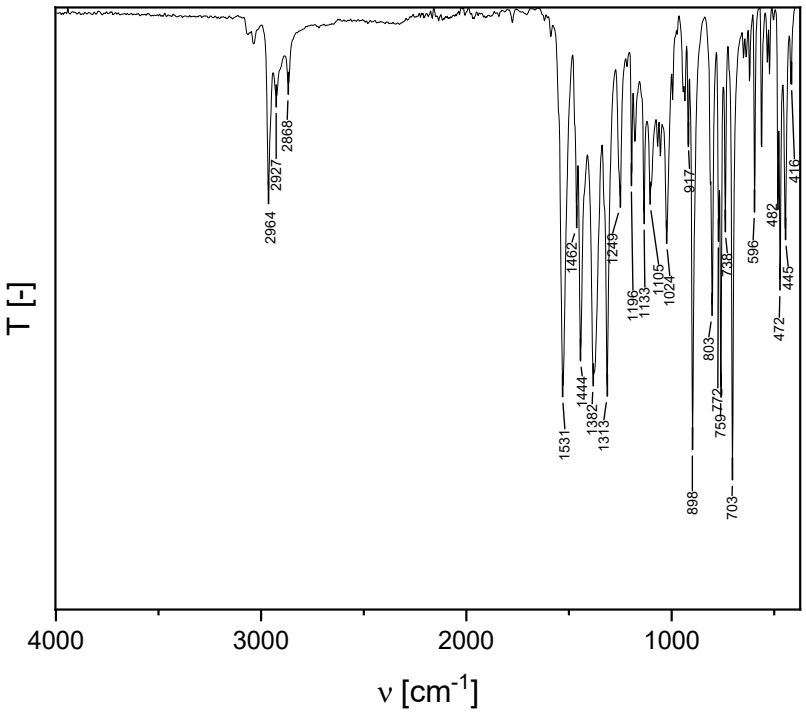

Fig. S13. ATR-IR spectrum of LAl ($C_{12}H_6O_2$) (**4**).

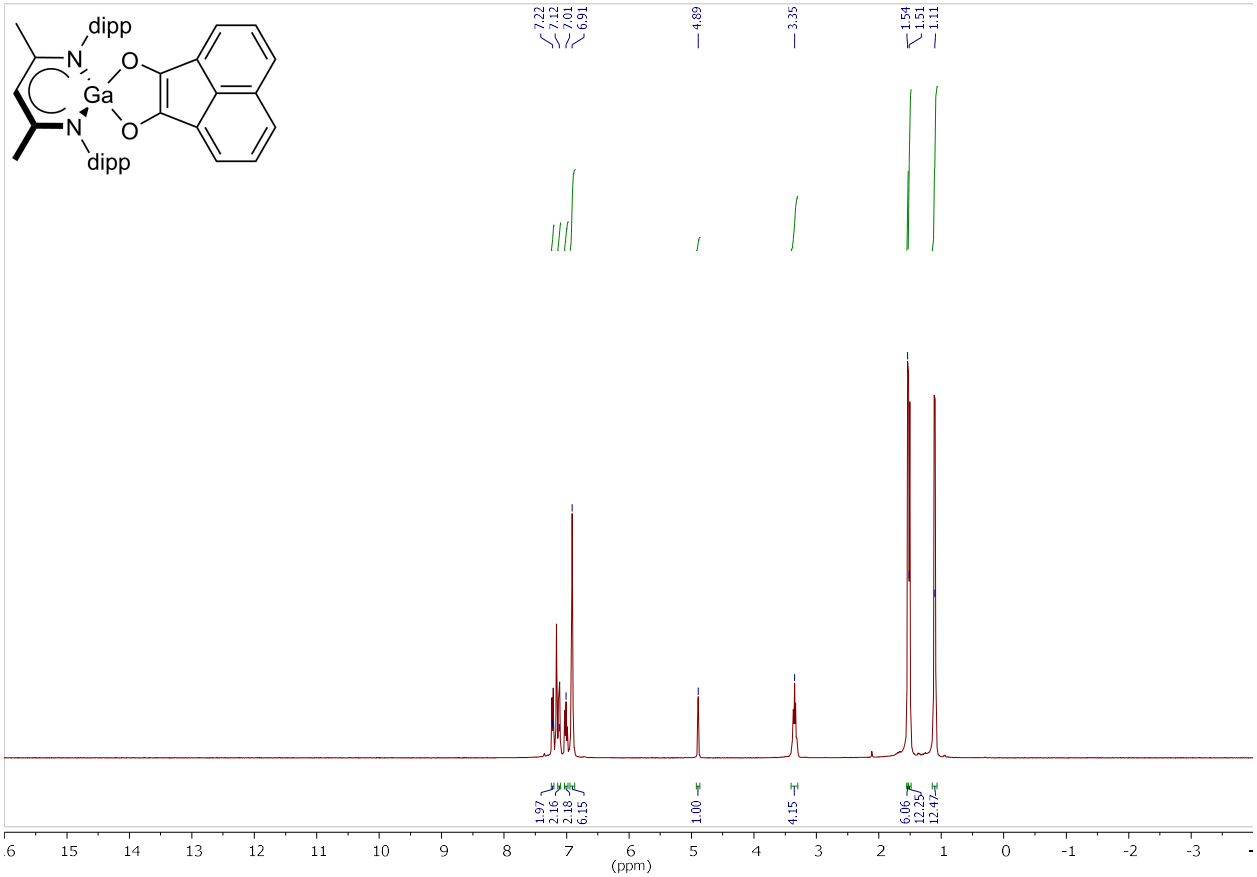

Fig. S14. ^{1}H NMR spectrum (400 MHz, C_6D_6, 25 °C) of LGa($C_{12}H_6O_2$) (**5**).

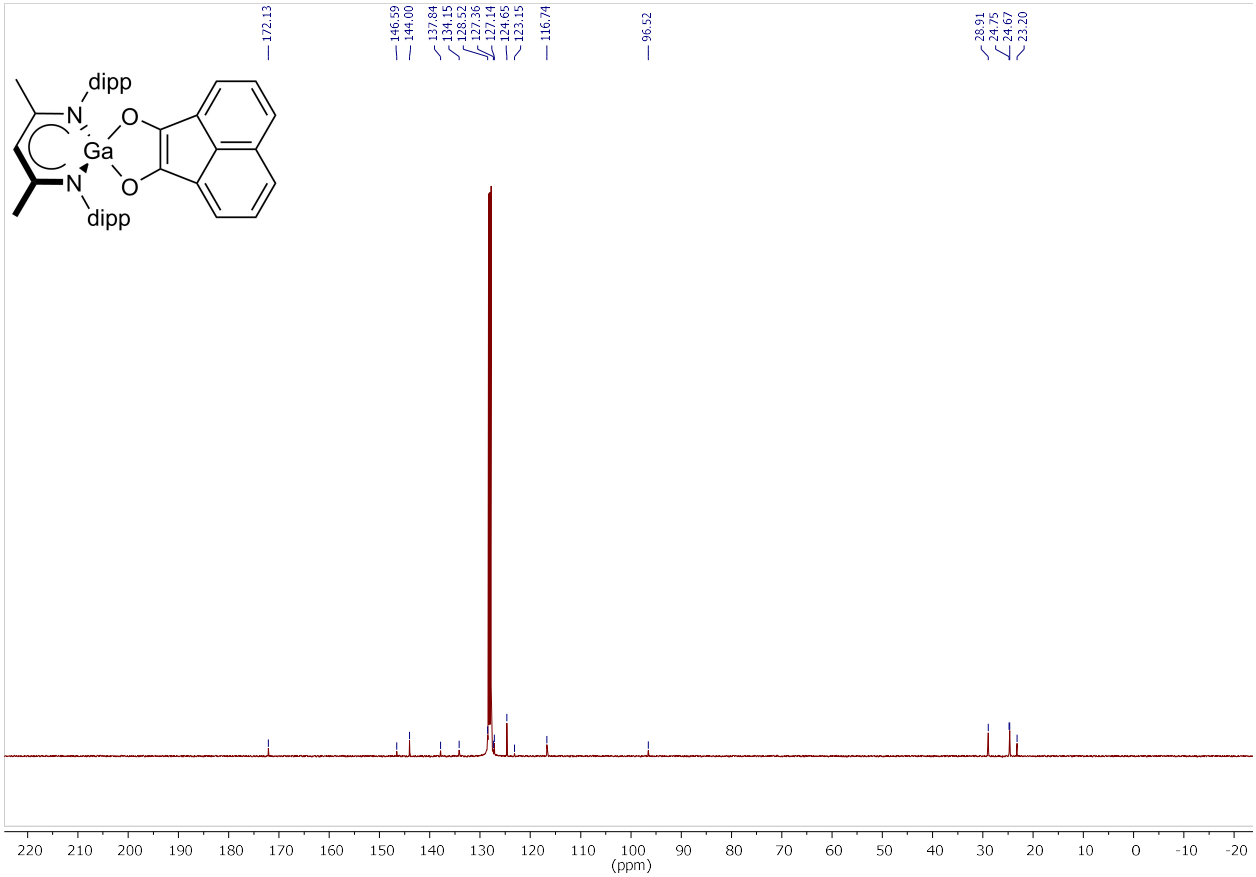

Fig. S15. ^{13}C NMR spectrum (100.6 MHz, C_6D_6, 25 °C) of LGa($C_{12}H_6O_2$) (**5**).

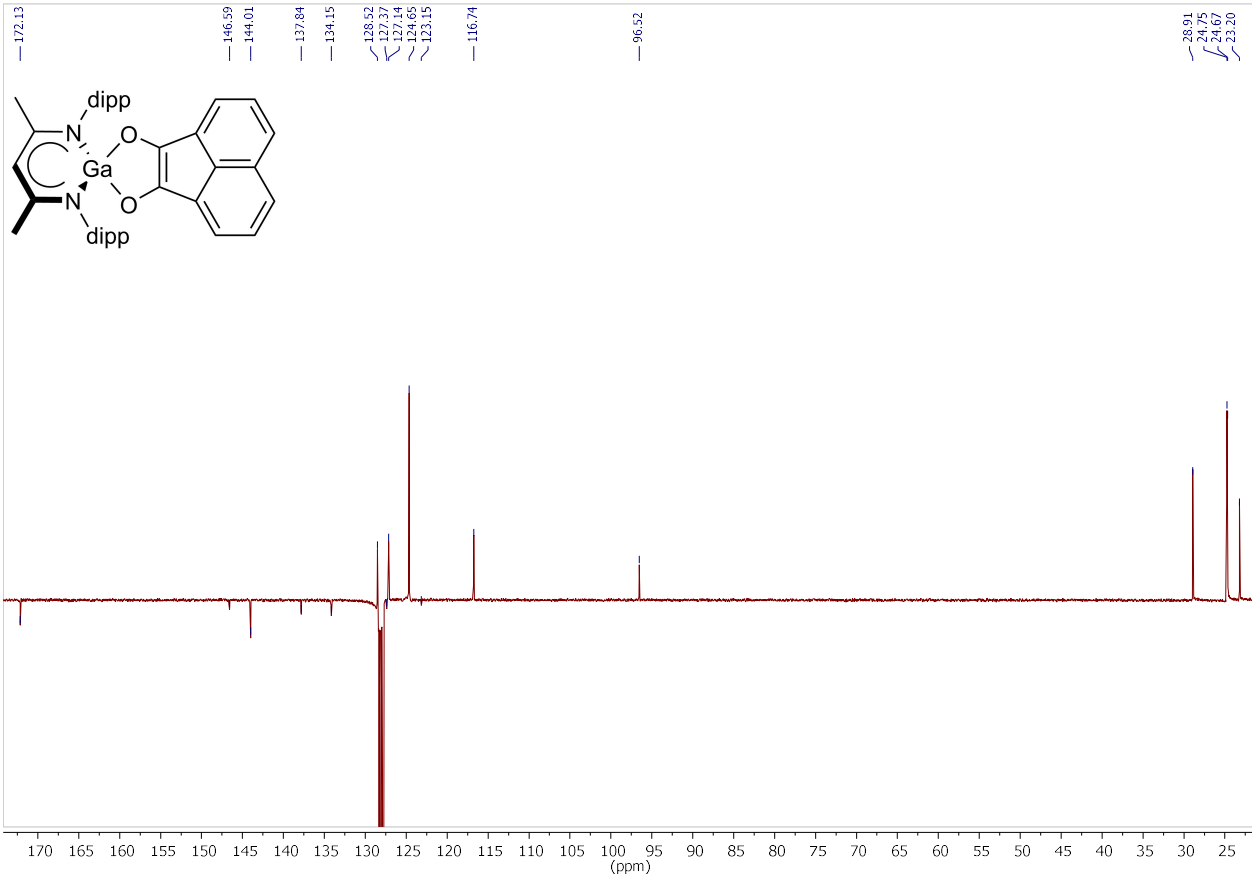

Fig. S16. DEPTQ ^{13}C NMR spectrum (100.6 MHz, C_6D_6, 25 °C) of LGa($C_{12}H_6O_2$) (**5**).

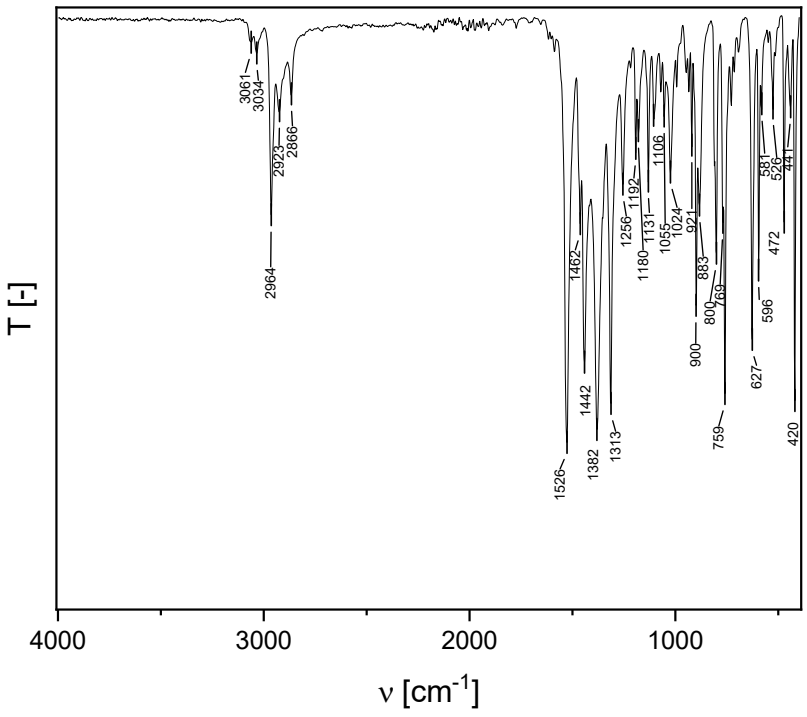

Fig. S17. ATR-IR spectrum of LGa($C_{12}H_6O_2$) (**5**).

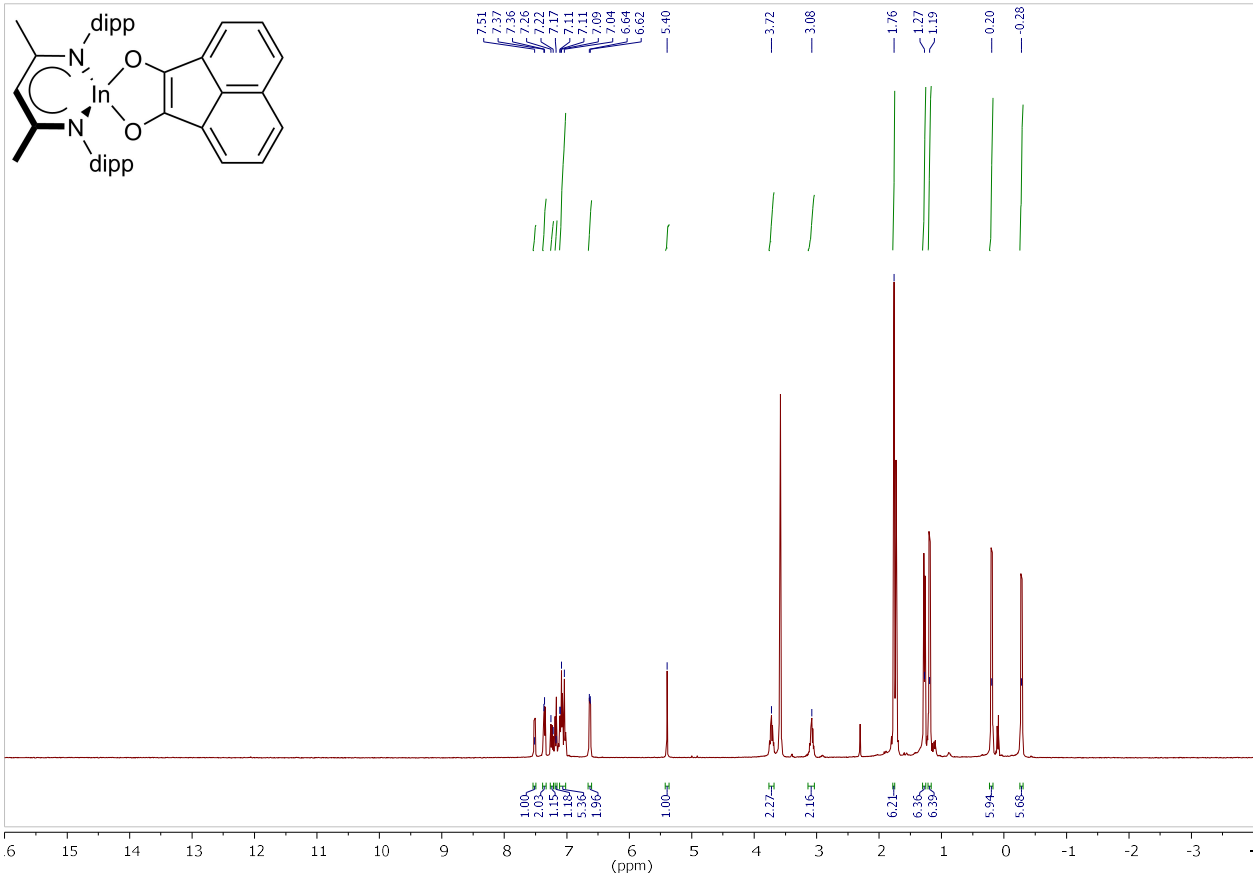

Fig. S18. ^{1}H NMR spectrum (400 MHz, thf-d_8, 25 °C) of LIn($C_{12}H_6O_2$) (**6**).

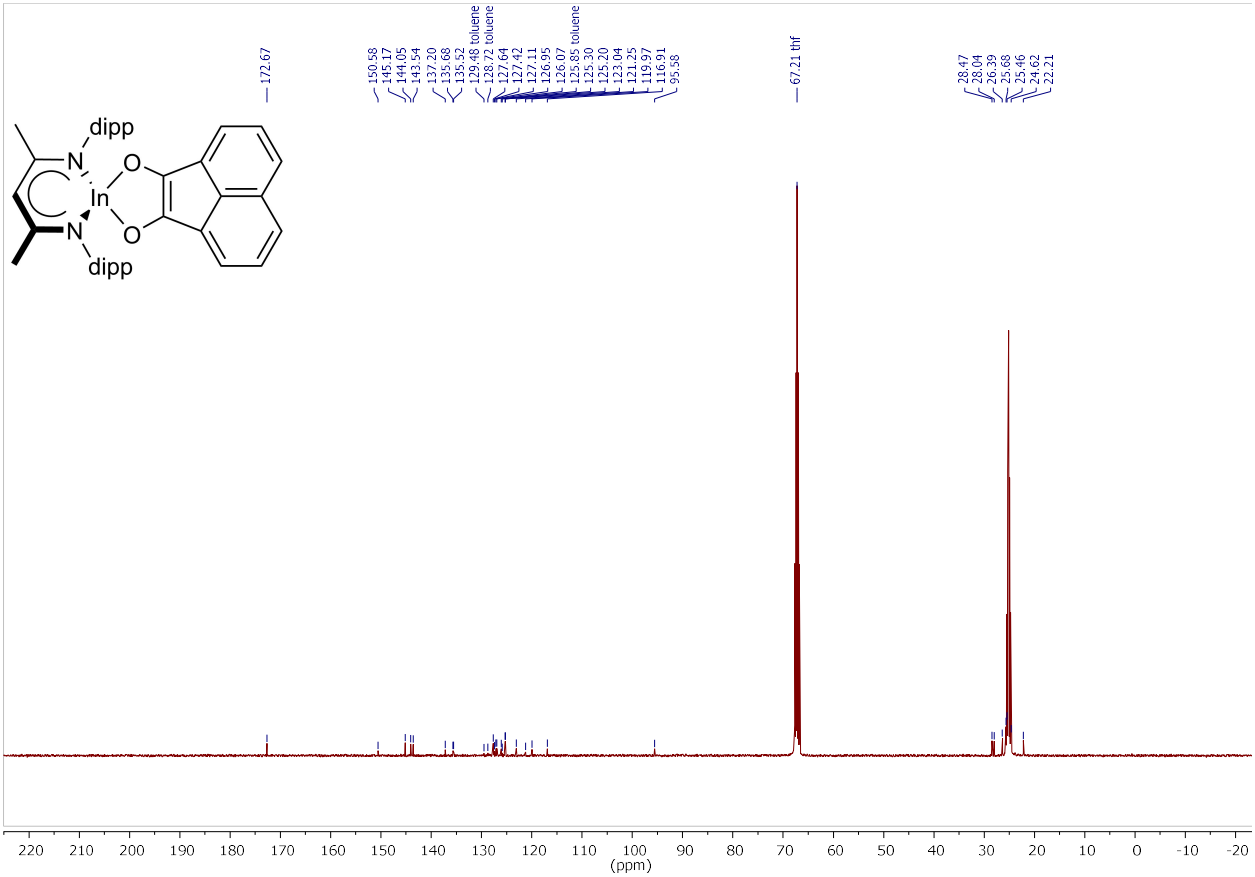

Fig. S19. ^{13}C NMR spectrum (100.6 MHz, thf-d_8, 25 °C) of LIn($C_{12}H_6O_2$) (**6**).

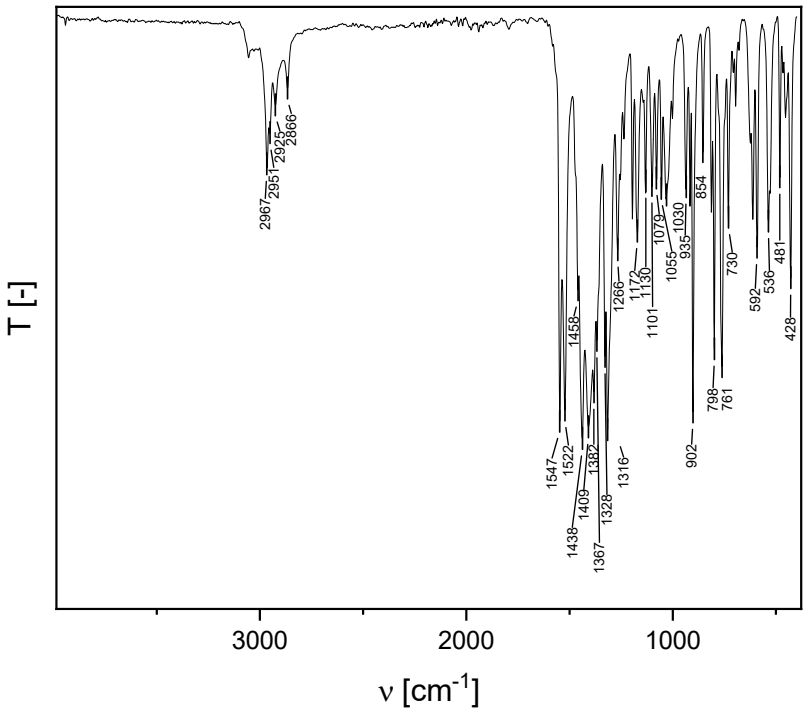

Fig. S20. ATR-IR spectrum of LIn($C_{12}H_6O_2$) (**6**).

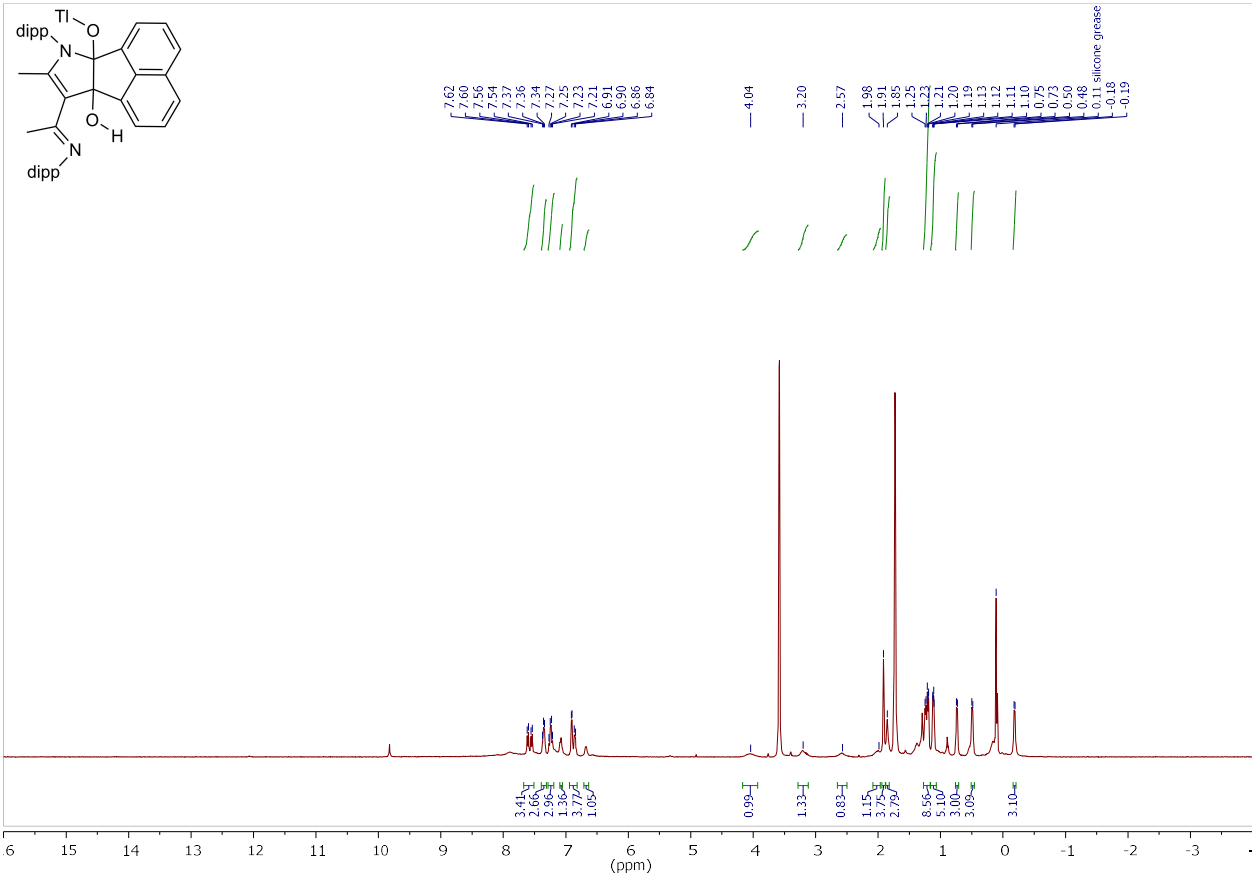

Fig. S21. ^{1}H NMR spectrum (400 MHz, C_6D_6, 25 °C) of the solid (**7**) obtained from the reaction of LTl with acenaphthenequinone.

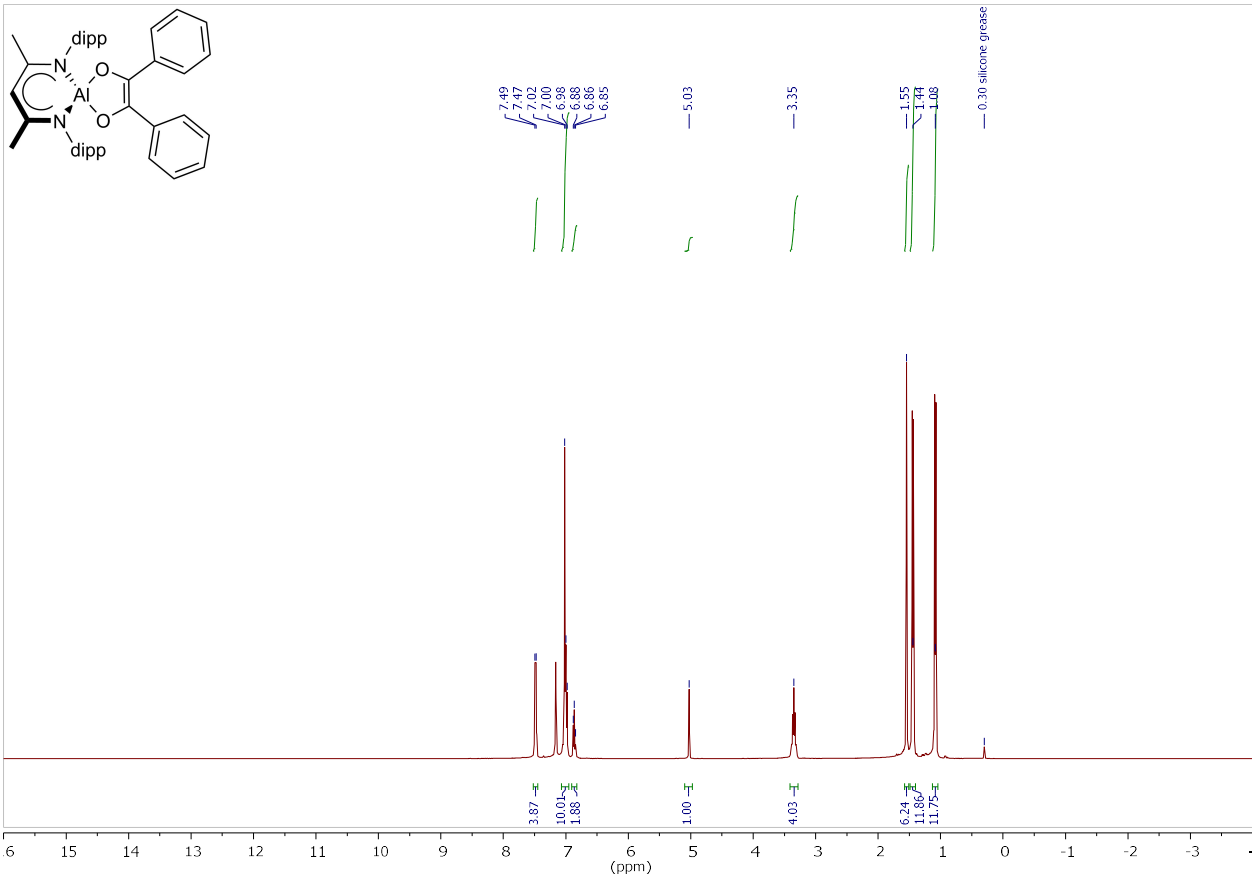

Fig. S22. ^{1}H NMR spectrum (400 MHz, C_6D_6, 25 °C) of LAl($C_{14}H_{10}O_2$) (**8**).

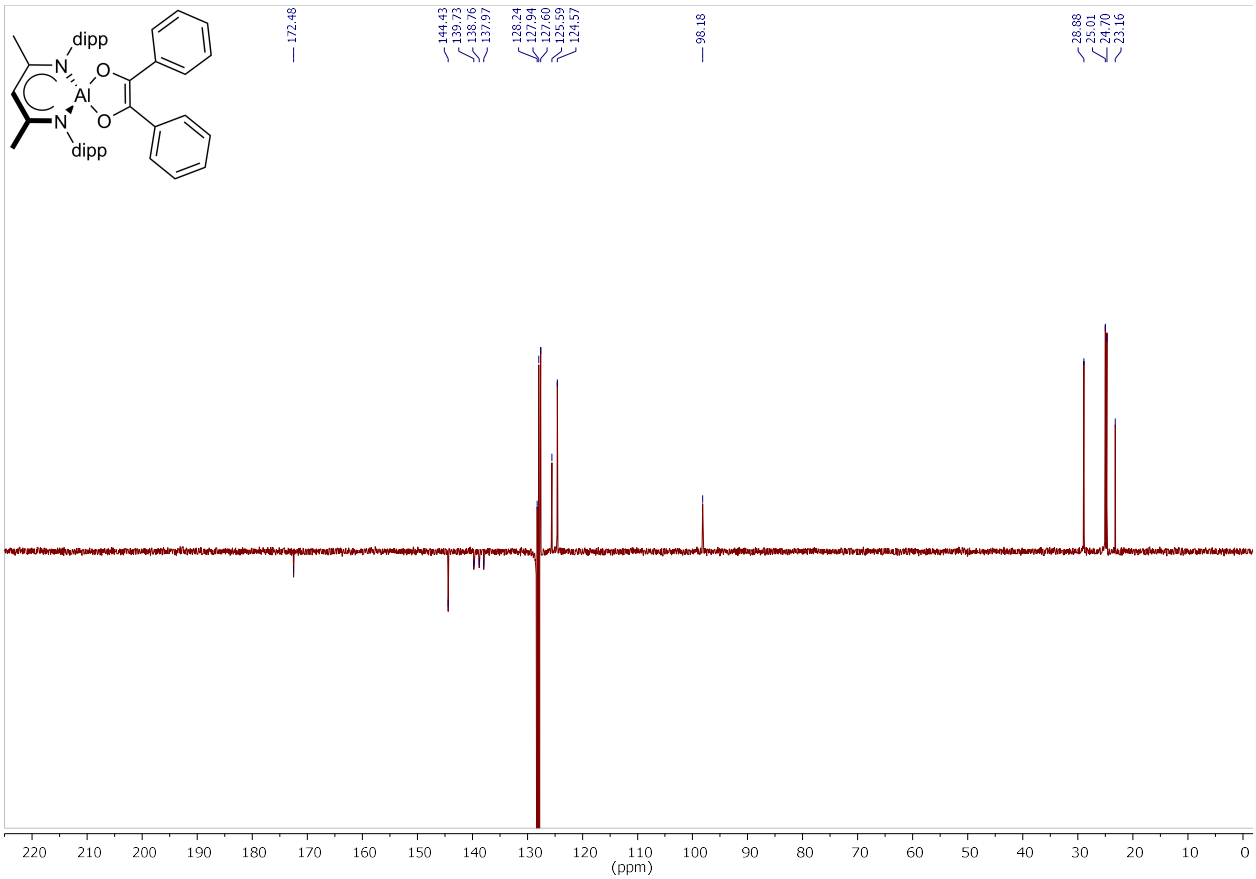

Fig. S23. DEPTQ ^{13}C NMR spectrum (100.6 MHz, C_6D_6, 25 °C) of $LAl(C_{14}H_{10}O_2)$ (**8**).

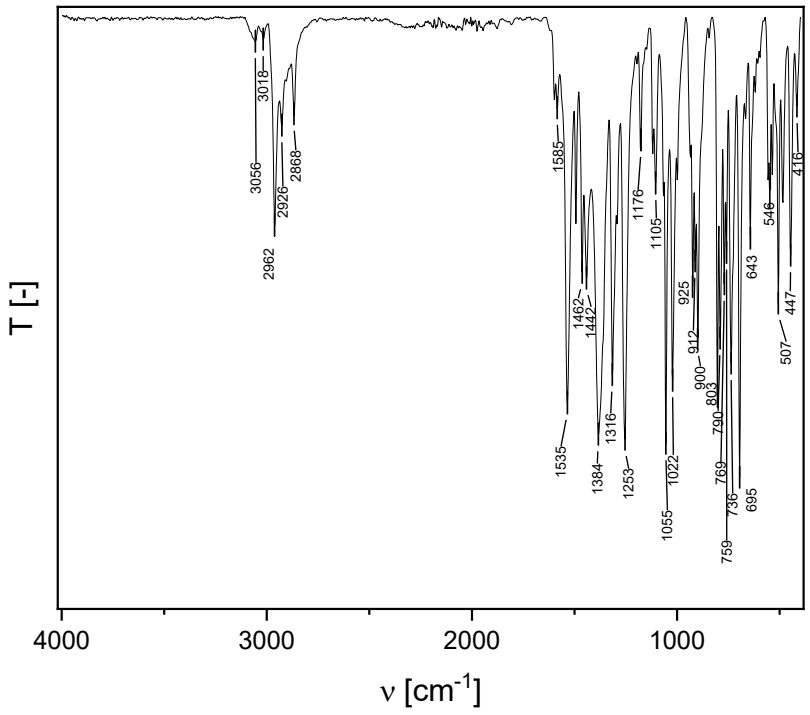

Fig. S24. ATR-IR spectrum of $LAl(C_{14}H_{10}O_2)$ (**8**).

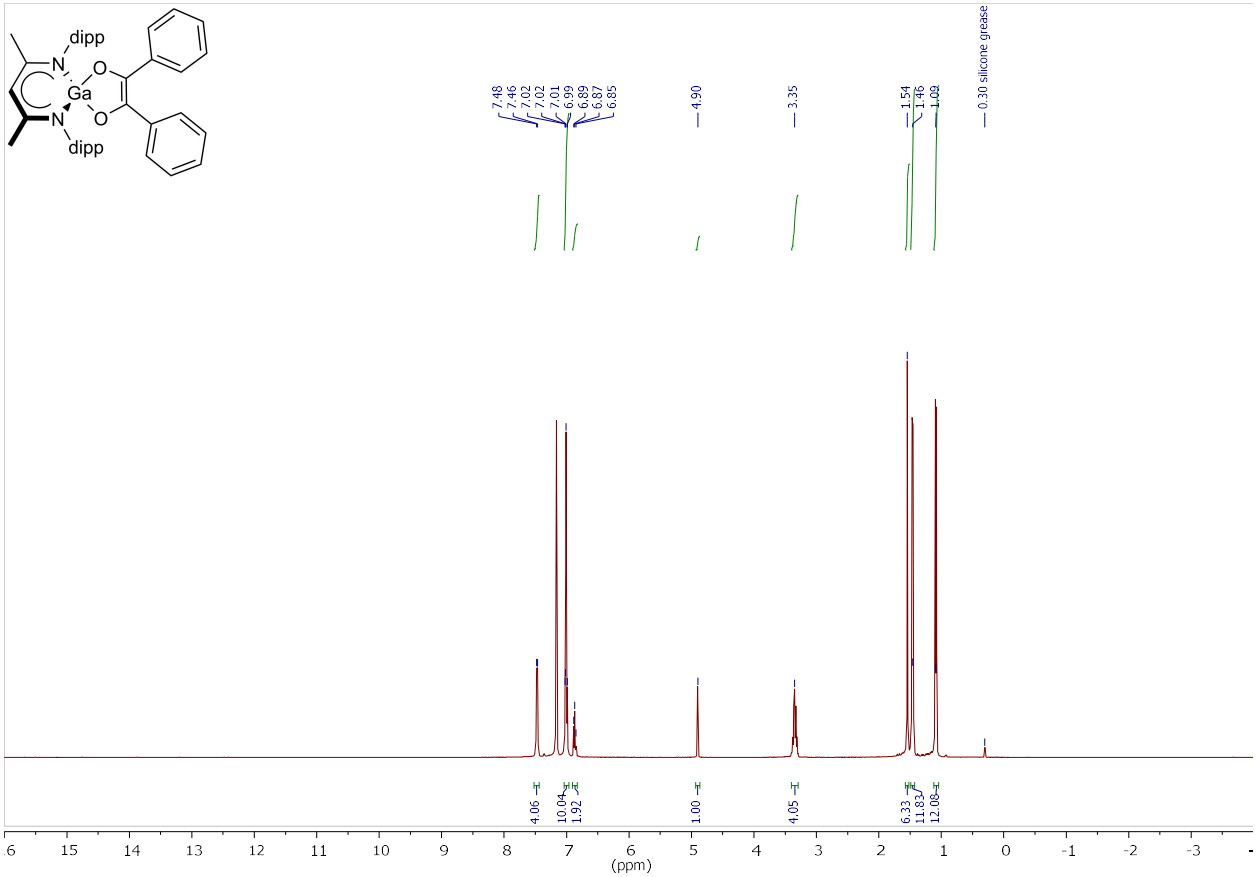

Fig. S25. ^{1}H NMR spectrum (400 MHz, C_6D_6, 25 °C) of LGa($C_{14}H_{10}O_2$) (**9**).

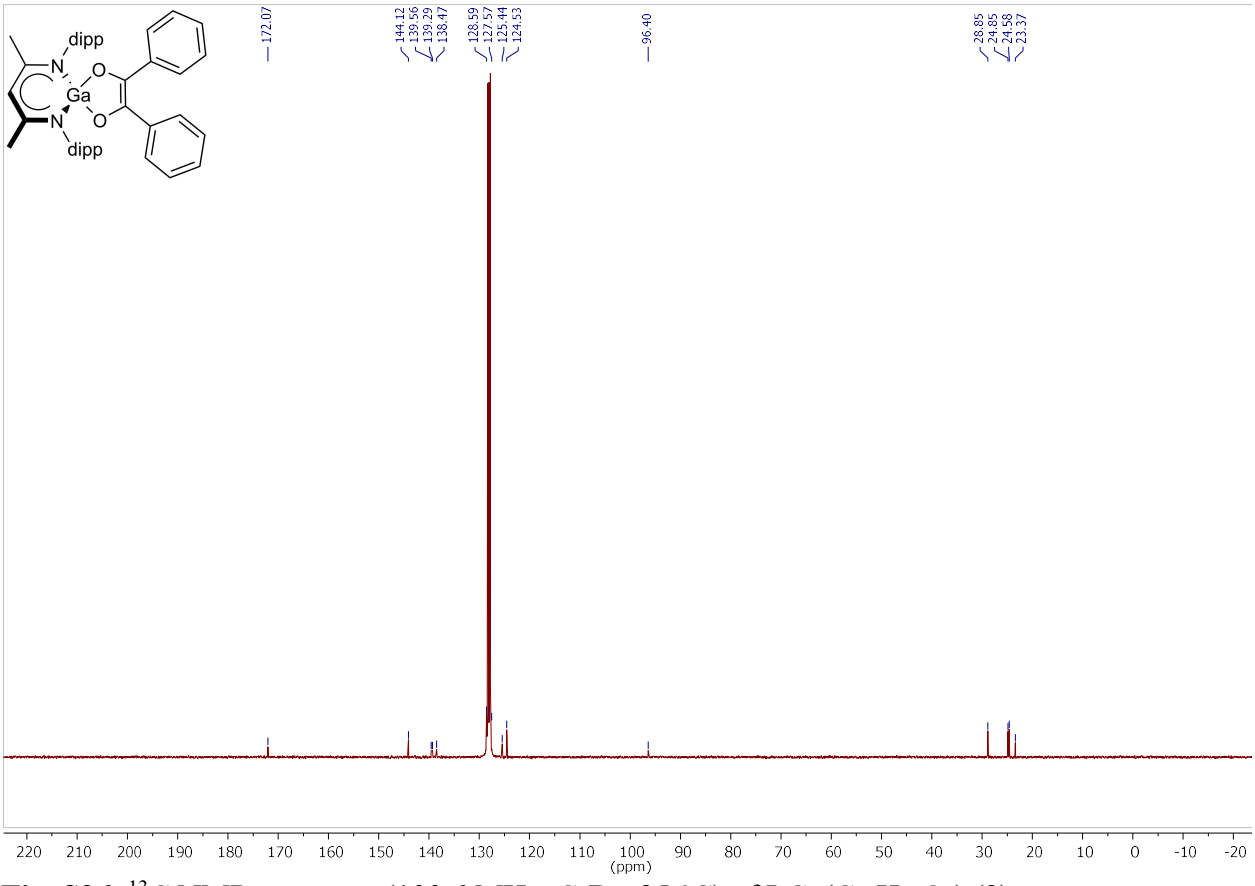

Fig. S26. ^{13}C NMR spectrum (100.6 MHz, C_6D_6, 25 °C) of LGa($C_{14}H_{10}O_2$) (**9**).

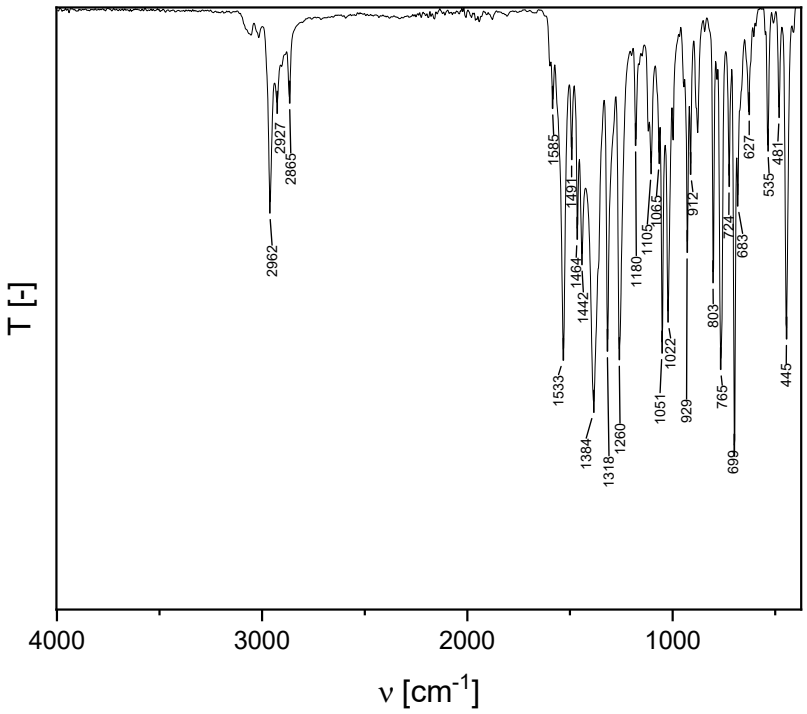

Fig. S27. ATR-IR spectrum of LGa($C_{14}H_{10}O_2$) (**9**).

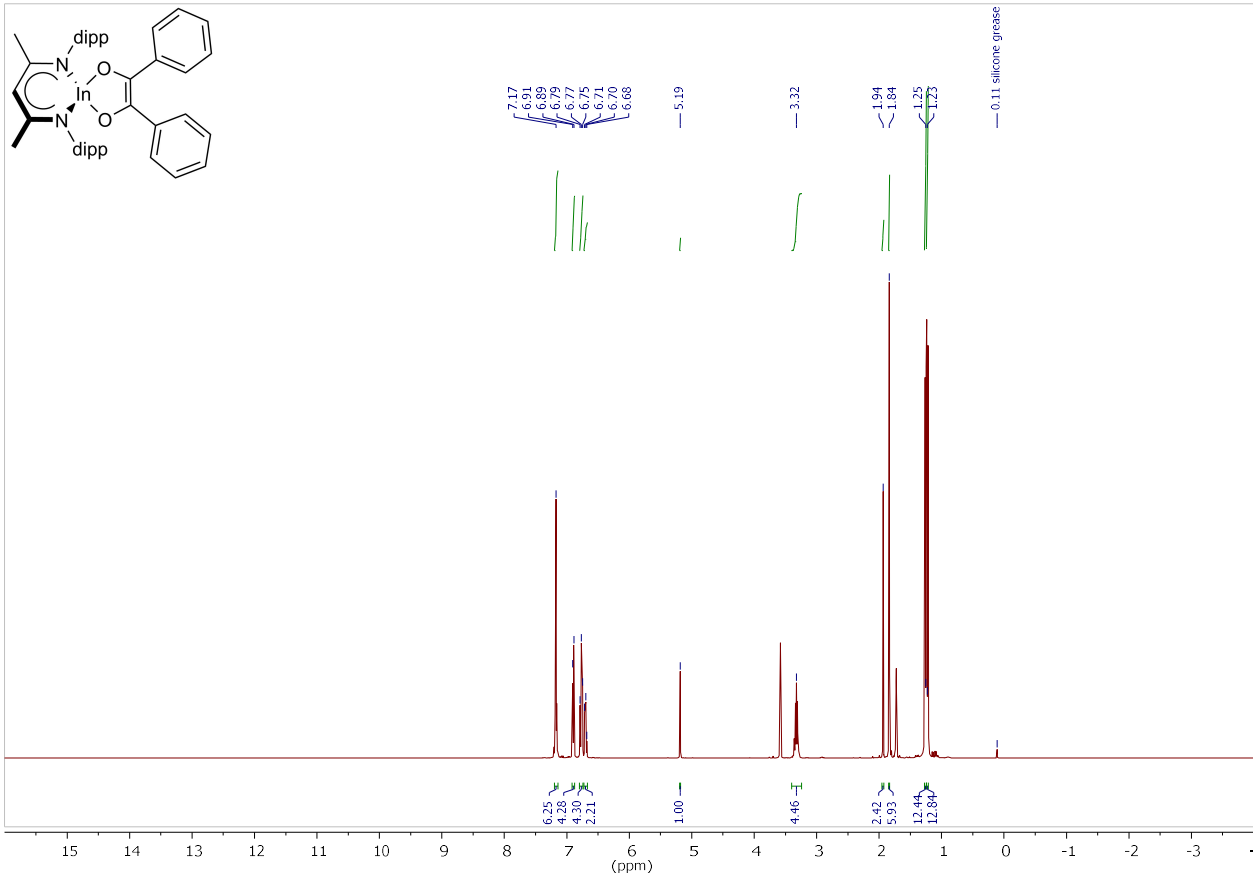

Fig. S28. ^{1}H NMR spectrum (400 MHz, thf-d_8, 25 °C) of LIn($C_{14}H_{10}O_2$)·MeCN (**10**).

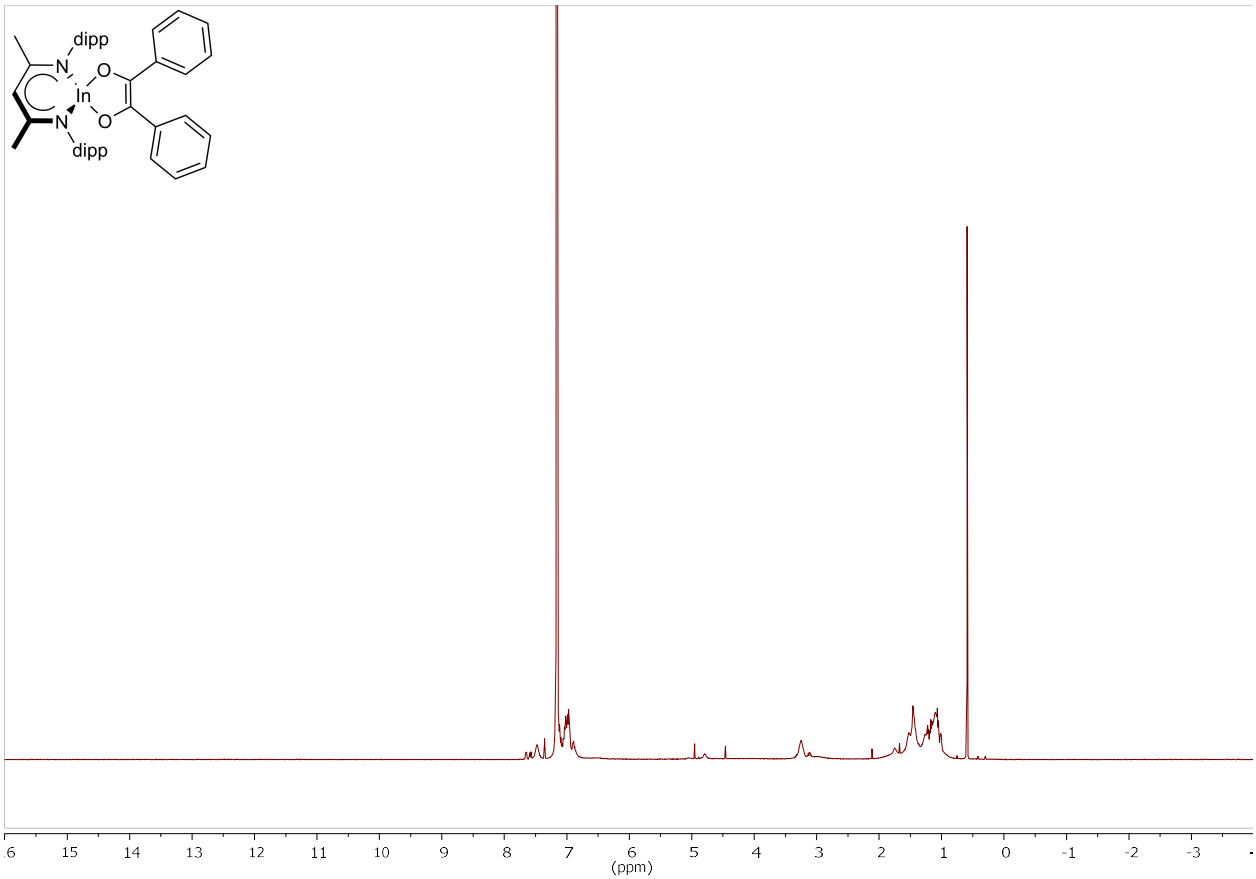

Fig. S29. ^{1}H NMR spectrum (400 MHz, C_6D_6, 25 °C) of $LIn(C_{14}H_{10}O_2)\cdot MeCN$ (**10**).

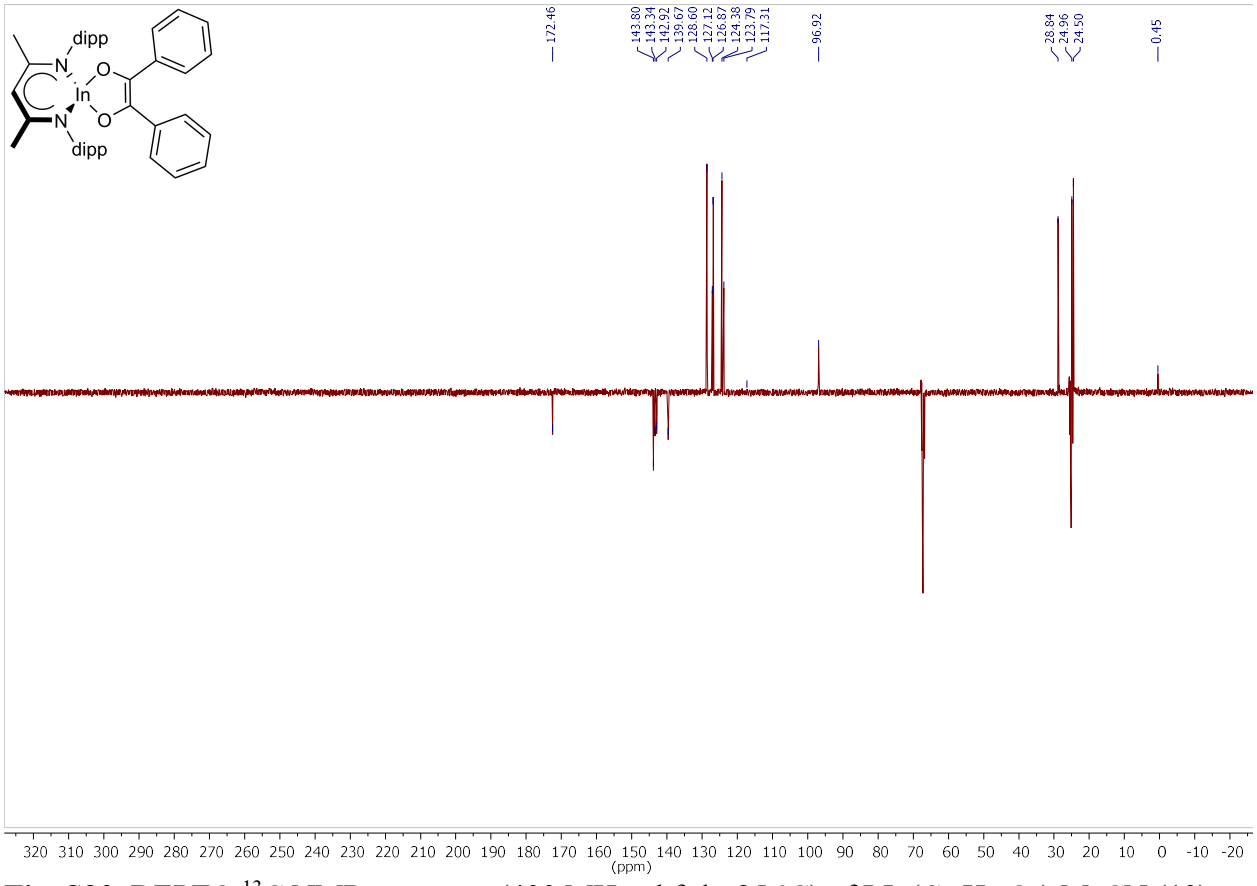

Fig. S30. DEPTQ ^{13}C NMR spectrum (400 MHz, thf-d_8, 25 °C) of $LIn(C_{14}H_{10}O_2)\cdot MeCN$ (**10**).

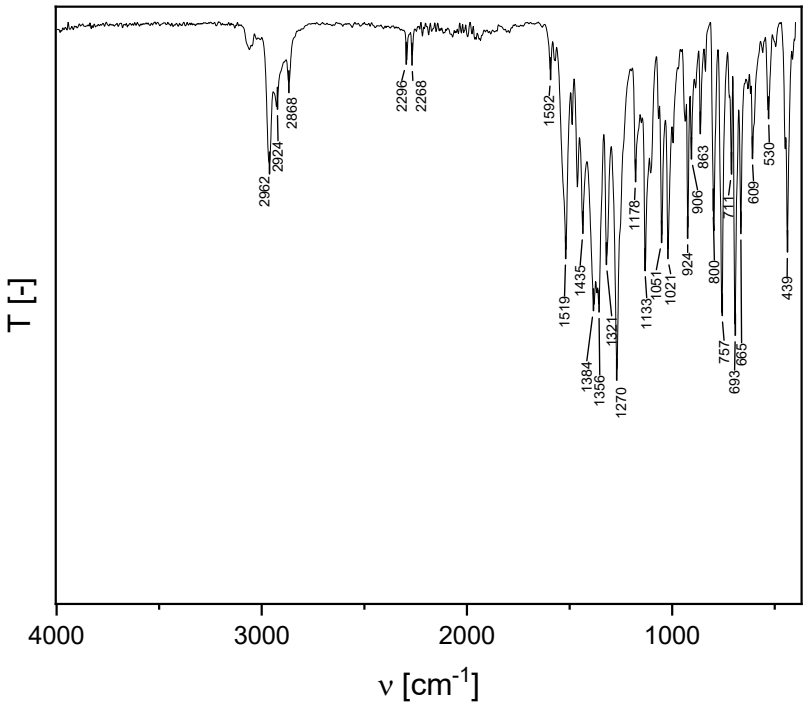

Fig. S31. ATR-IR spectrum of LIn($C_{14}H_{10}O_2$) MeCN (**10**).

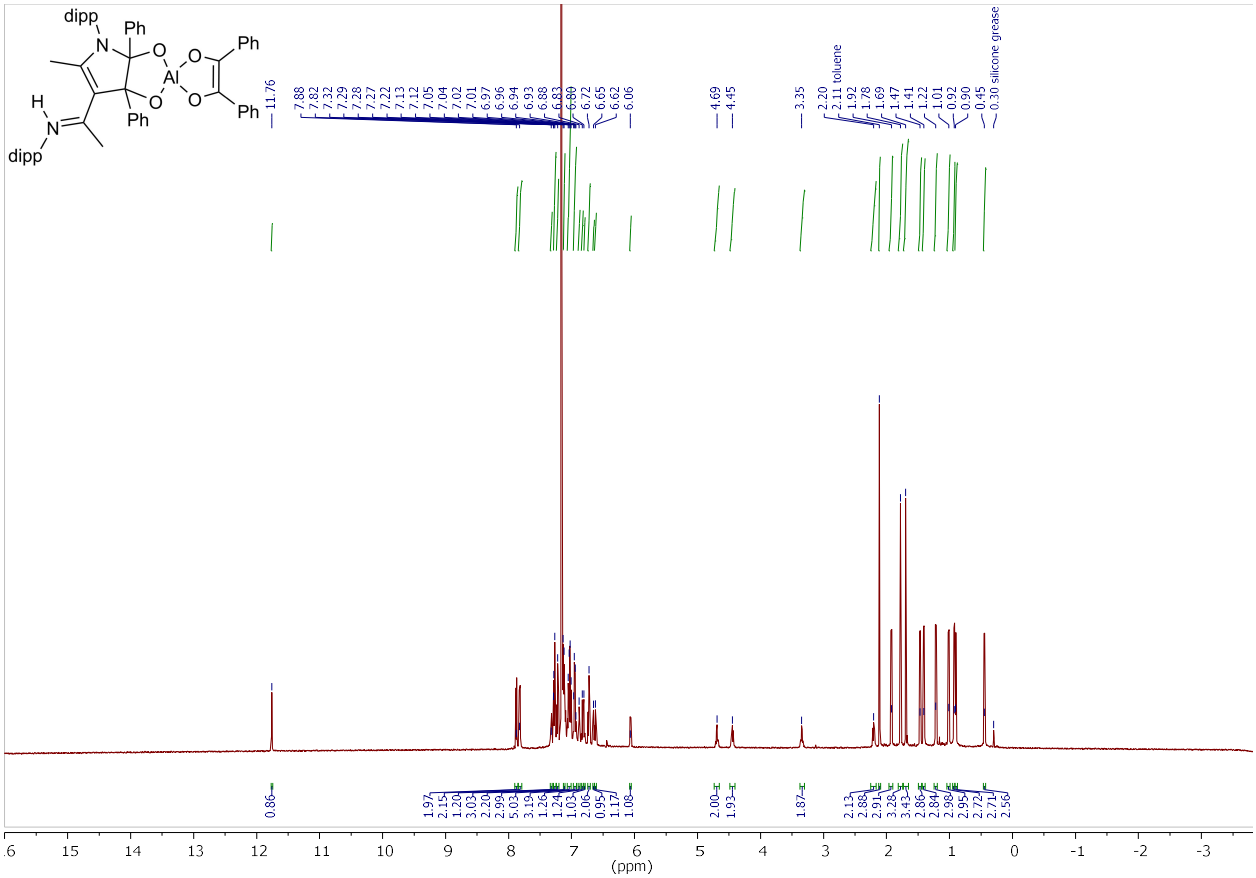

Fig. S32. ^{1}H NMR spectrum (400 MHz, C_6D_6, 25 °C) of LAl($C_{14}H_{10}O_2$)$_2$ (**11**).

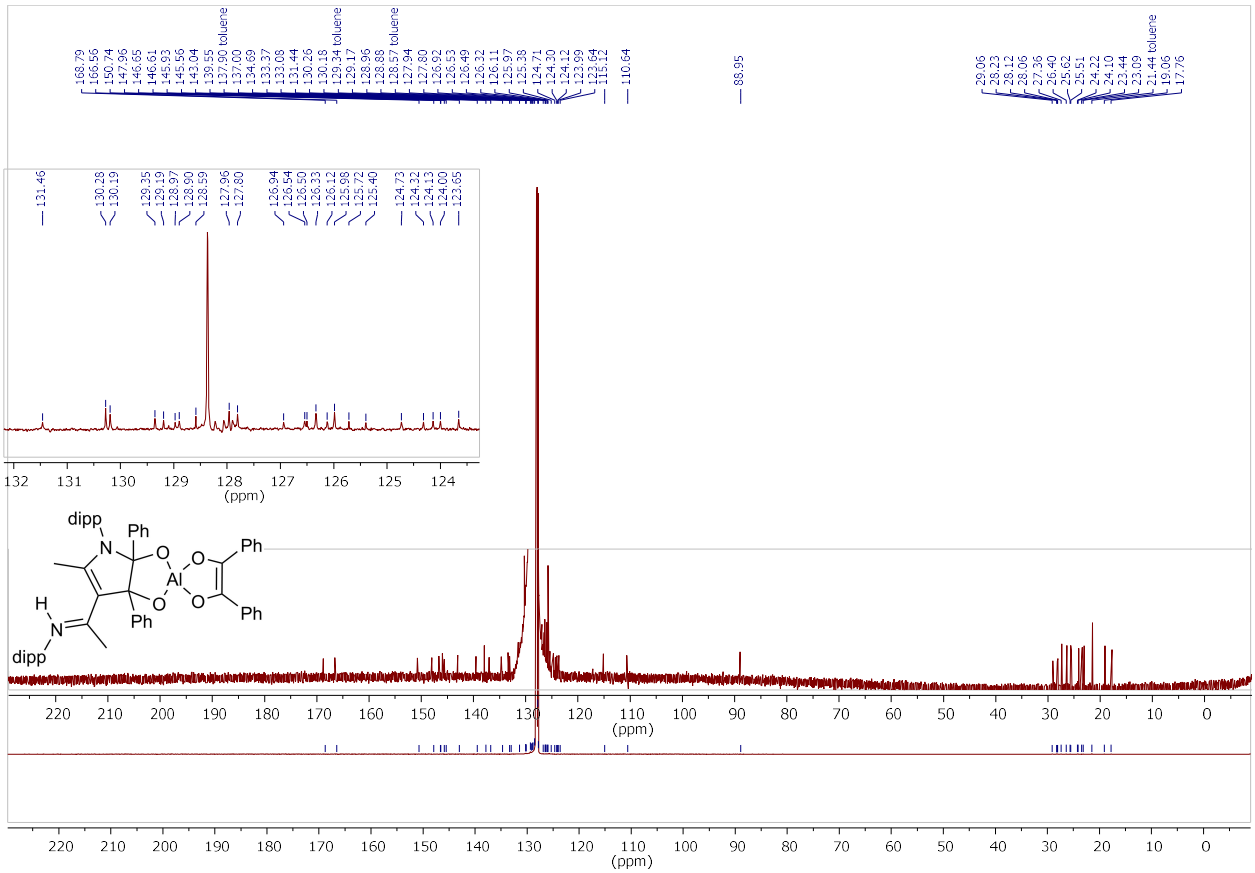

Fig. S33. ^{13}C NMR + 135DEPT spectrum (150.9 MHz, C_6D_6, 25 °C) of $LAl(C_{14}H_{10}O_2)_2$ (**11**).

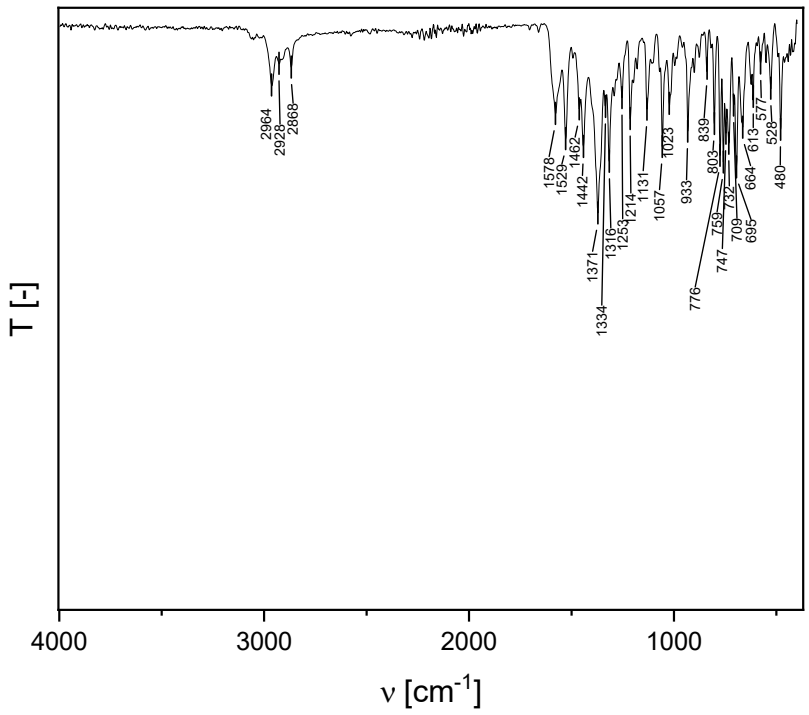

Fig. S 34. ATR-IR spectrum of $LAl(C_{14}H_{10}O_2)_2$ (**11**).

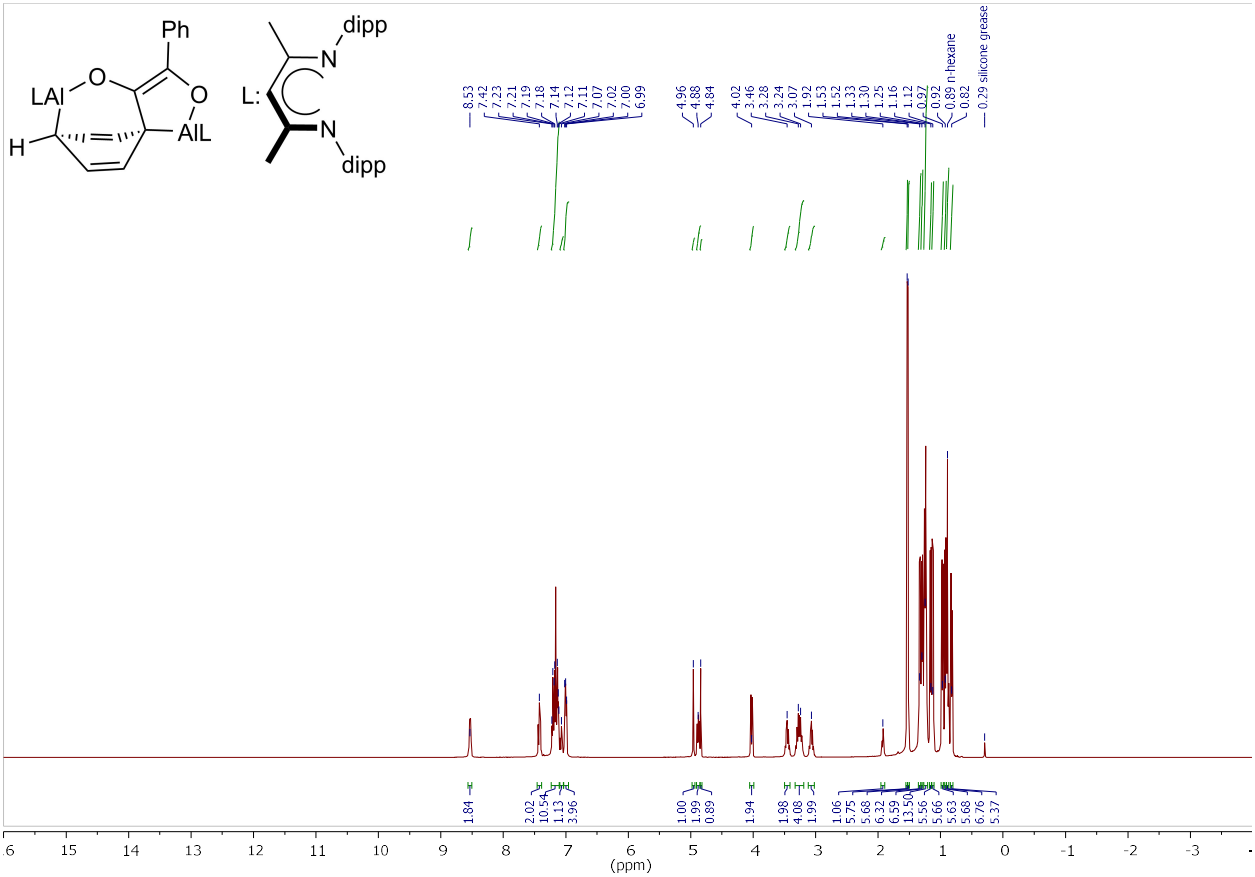

Fig. S35. ^{1}H NMR spectrum (400 MHz, C_6D_6, 25 °C) of $(LAl)_2(C_{14}H_{10}O_2)$ (**12**).

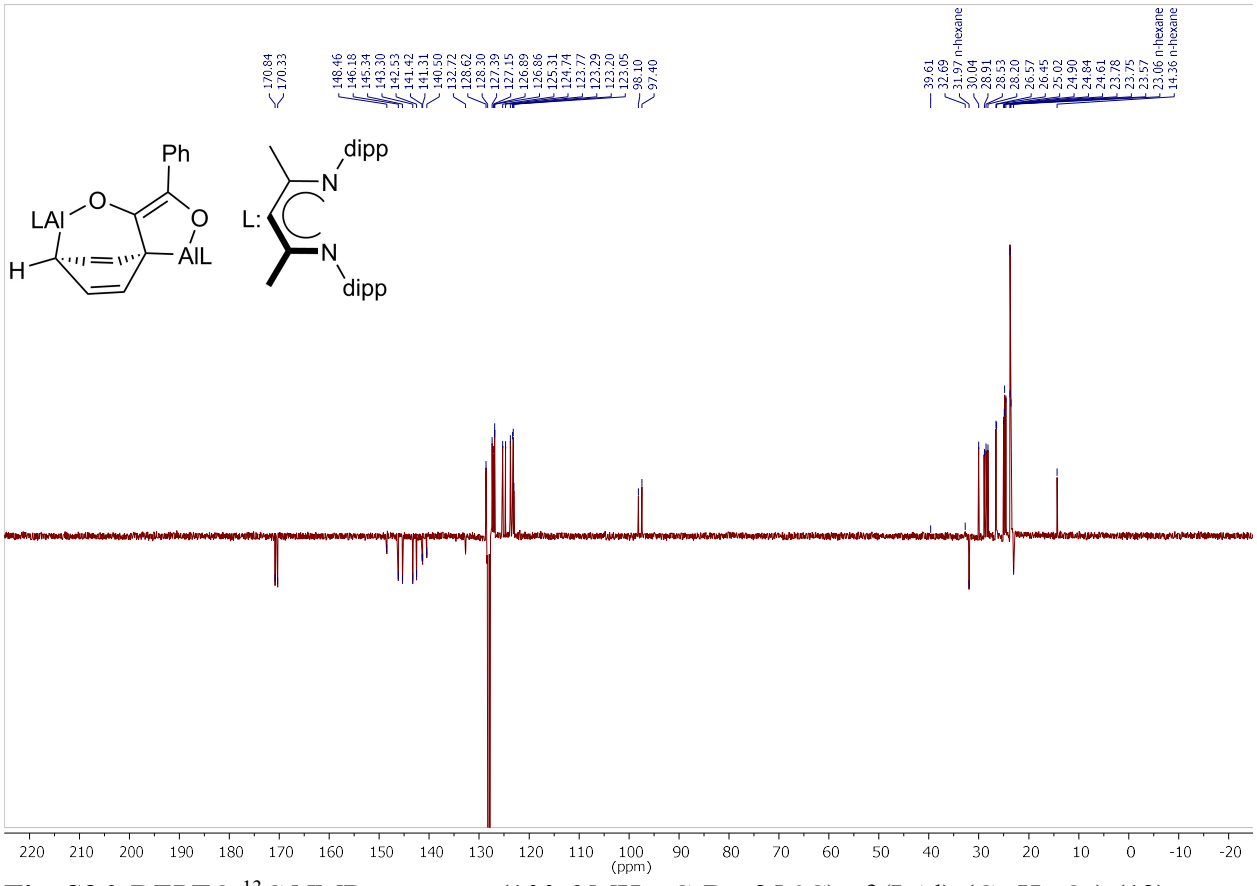

Fig. S36. DEPTQ ^{13}C NMR spectrum (100.6 MHz, C_6D_6, 25 °C) of $(LAl)_2(C_{14}H_{10}O_2)$ (**12**).

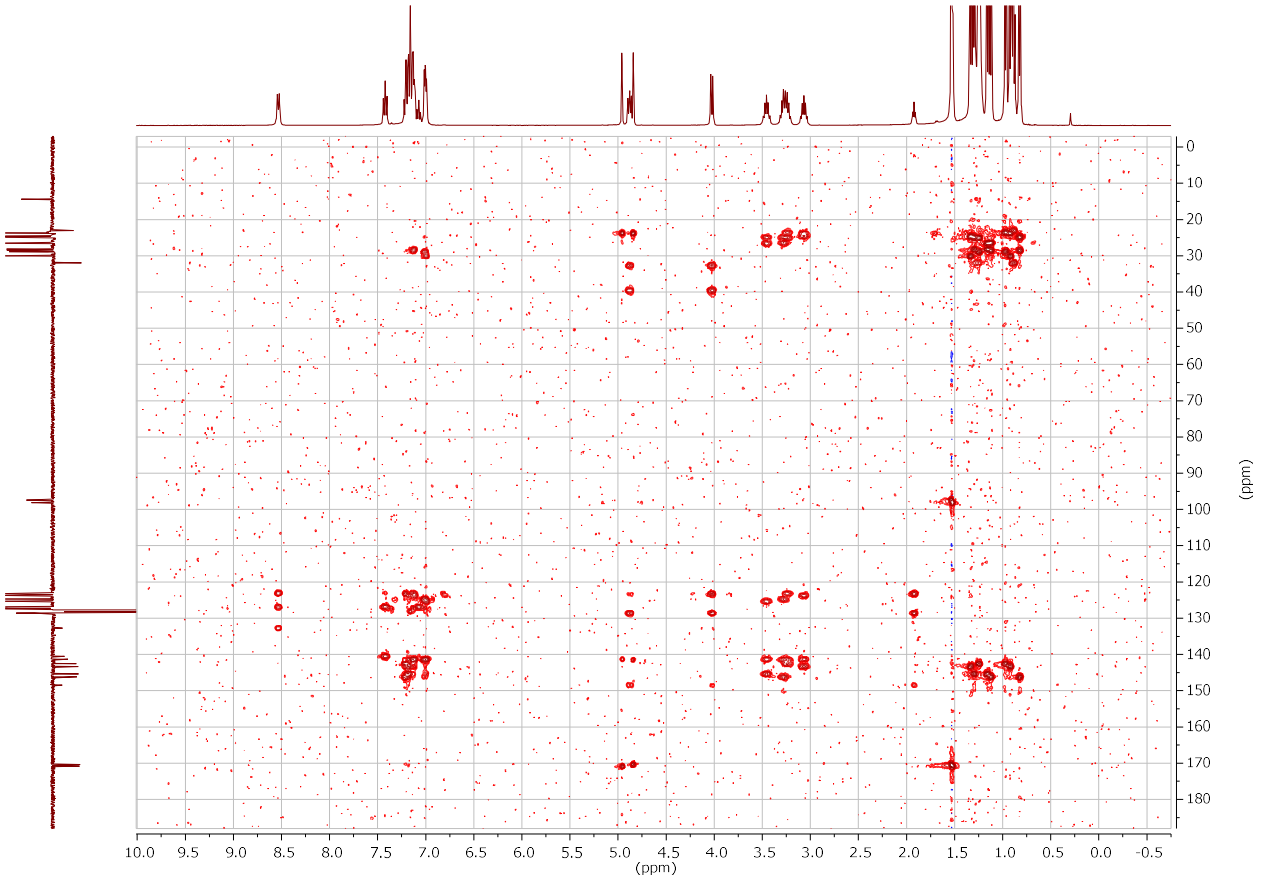

Fig. S37. HMBC spectrum (400/100.6 MHz, C_6D_6, 25 °C) of $(LAl)_2(C_{14}H_{10}O_2)$ (**12**).

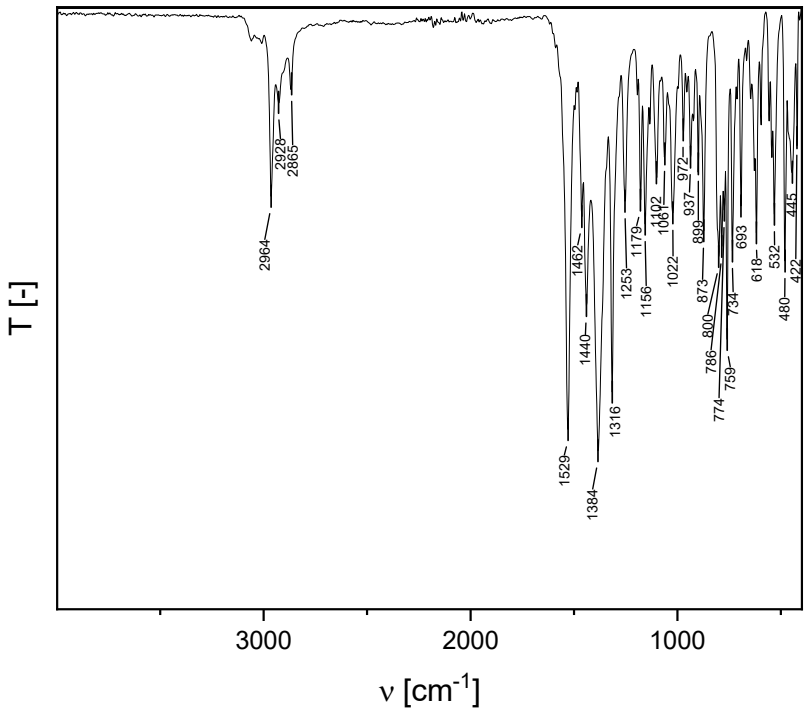

Fig. S38. ATR-IR spectrum of $(LAl)_2(C_{14}H_{10}O_2)$ (**12**).

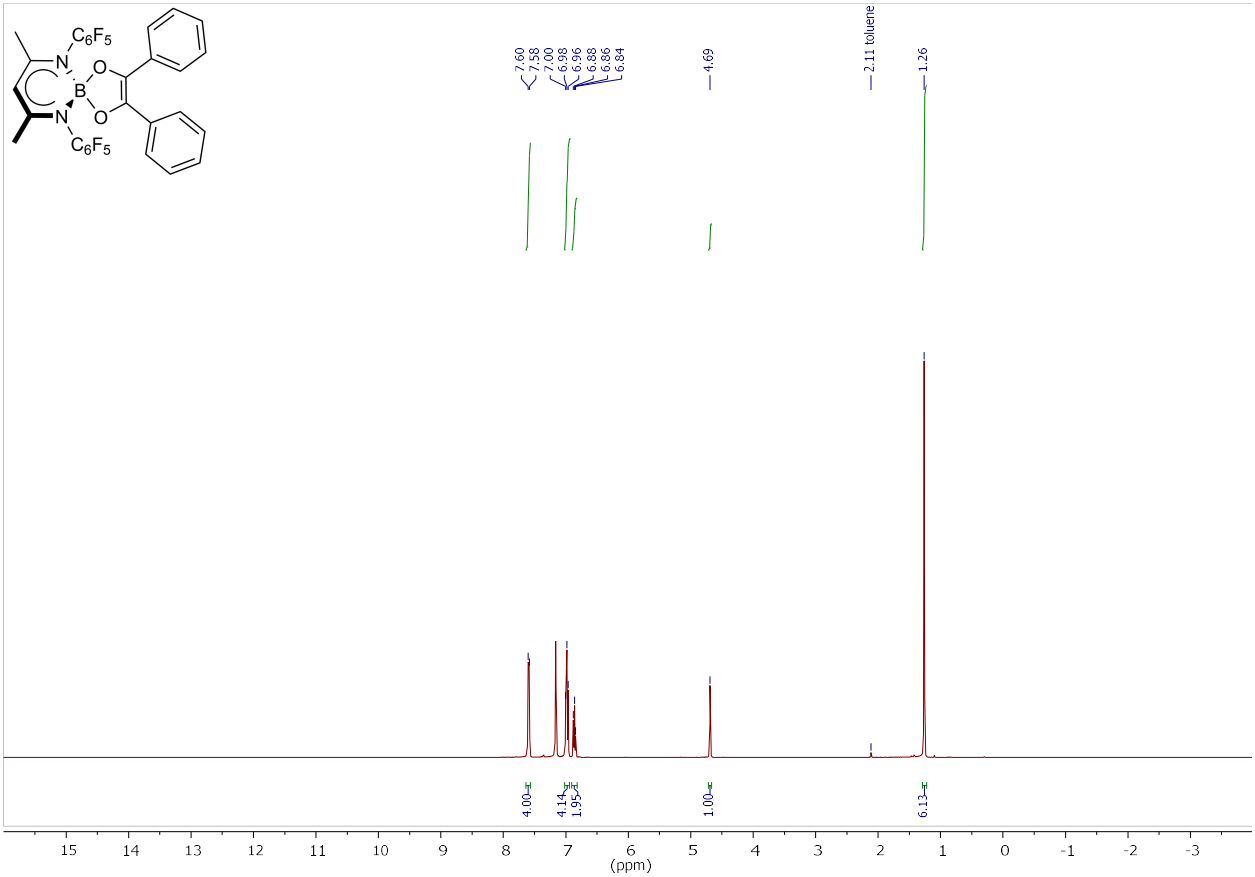

Fig. S39. ^{1}H NMR spectrum (400 MHz, C_6D_6, 25 °C) of L'B($C_{14}H_{10}O_2$) (**13**).

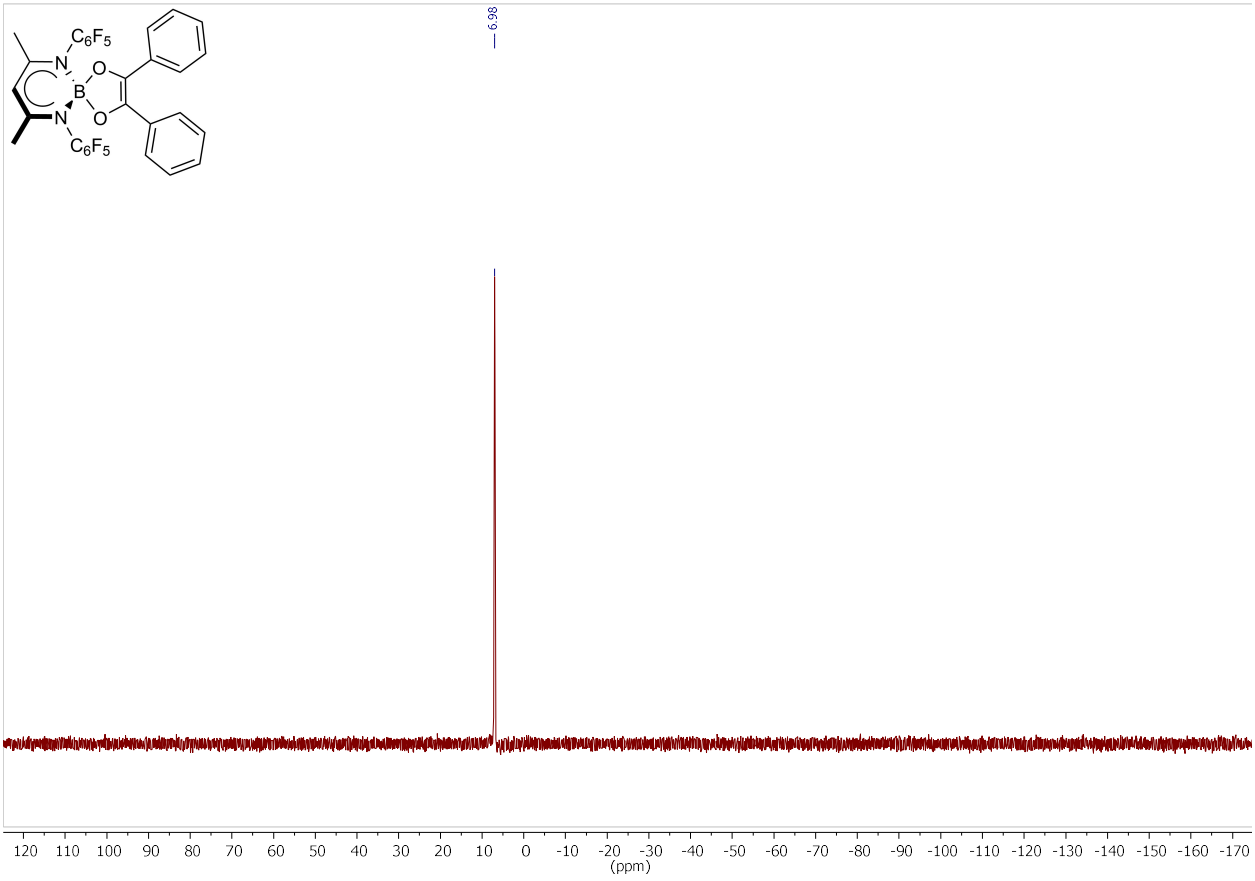

Fig. S40. ^{11}B NMR spectrum (128.4 MHz, C_6D_6, 25 °C) of L'B($C_{14}H_{10}O_2$) (**13**).

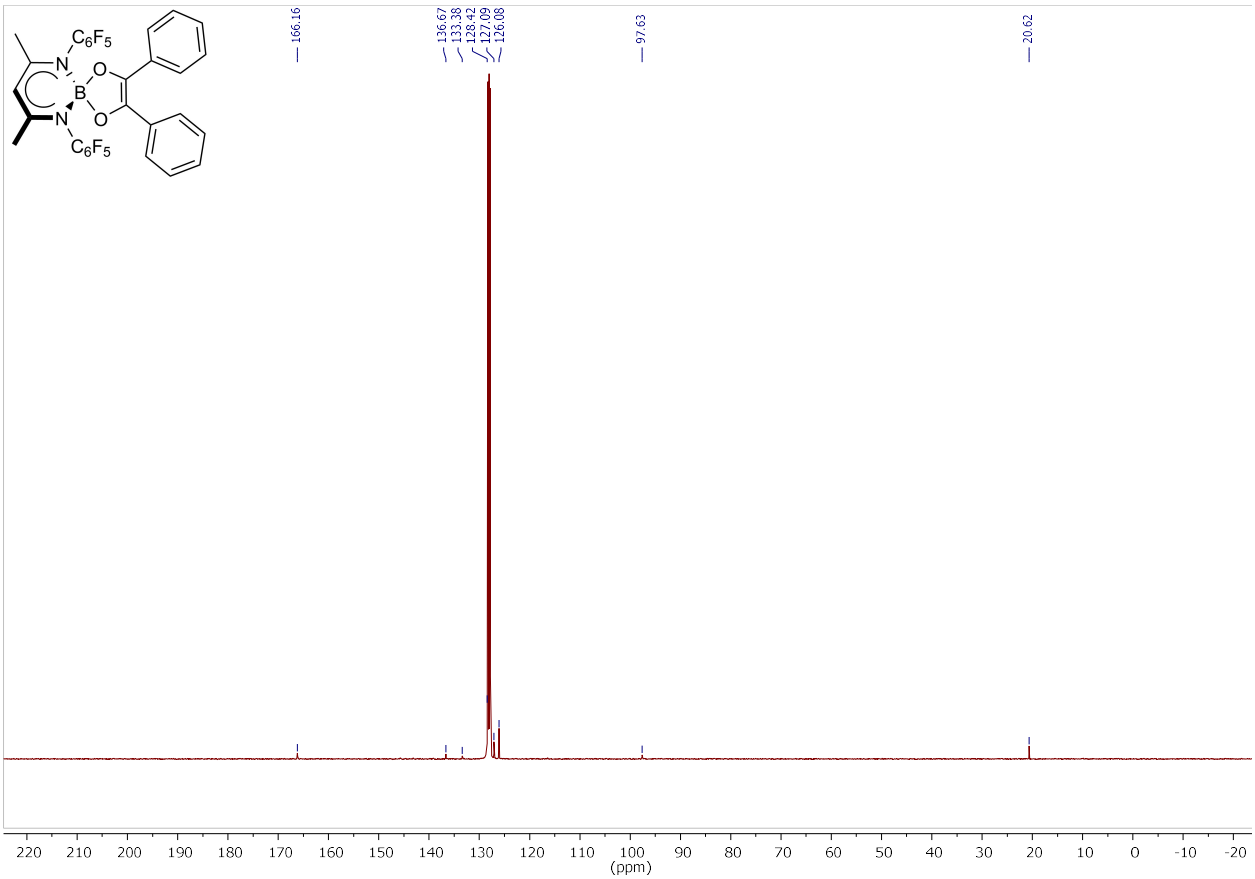

Fig. S41. ^{13}C NMR spectrum (100.6 MHz, C_6D_6, 25 °C) of L'B($C_{14}H_{10}O_2$) (**13**).

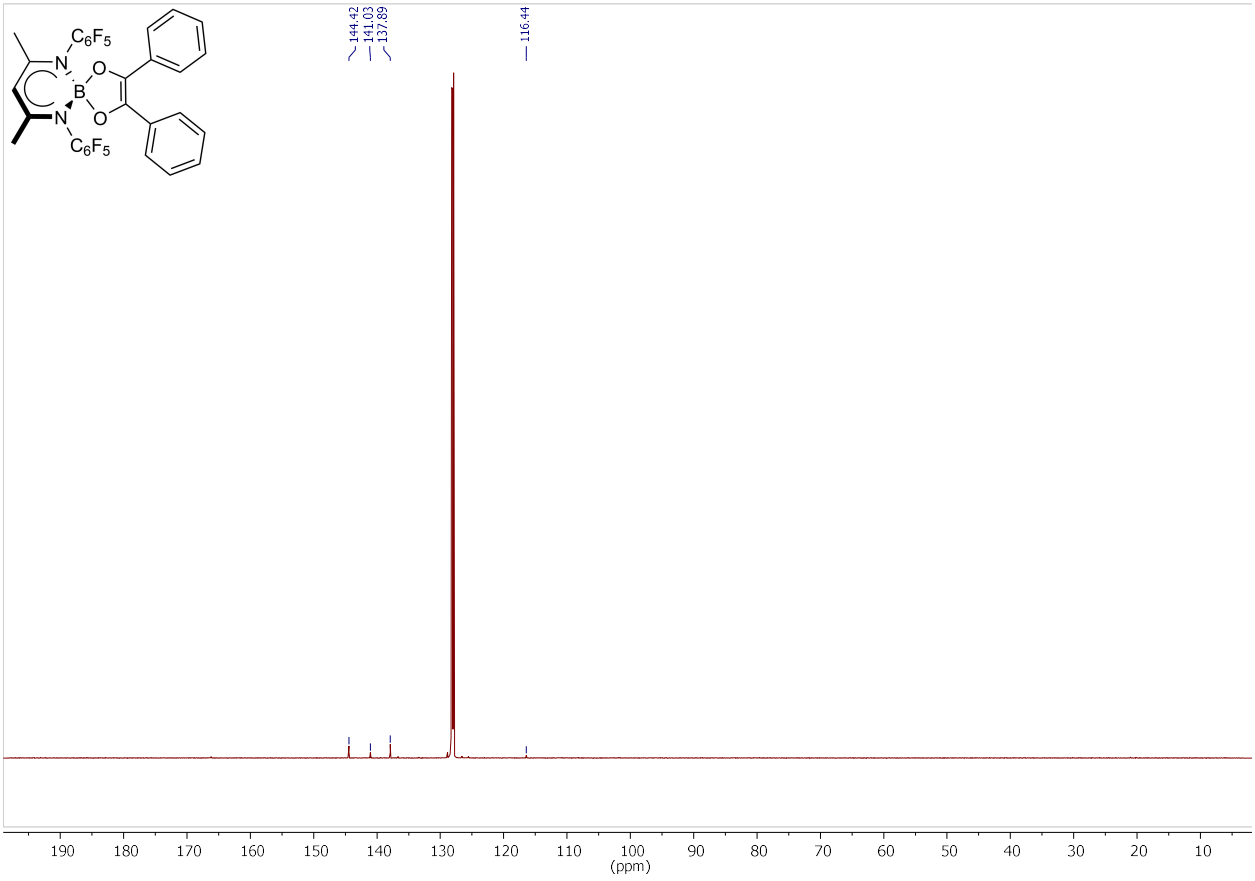

Fig. S42. ^{13}C {^{19}F} NMR spectrum (150.9 MHz, C_6D_6, 25 °C) of L'B($C_{14}H_{10}O_2$) (**13**).

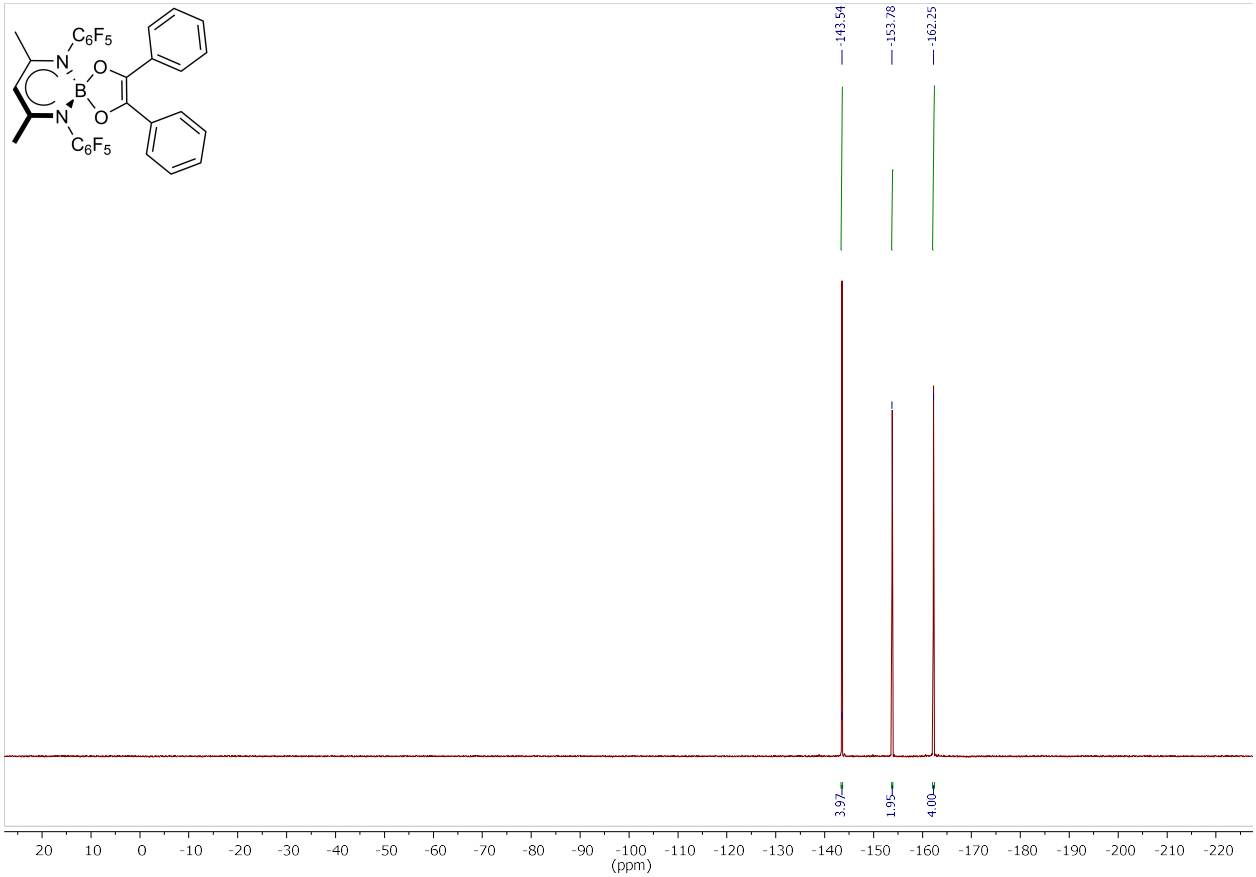

Fig. S43. ^{19}F NMR spectrum (376.5 MHz, C_6D_6, 25 °C) of L'B($C_{14}H_{10}O_2$) (**13**).

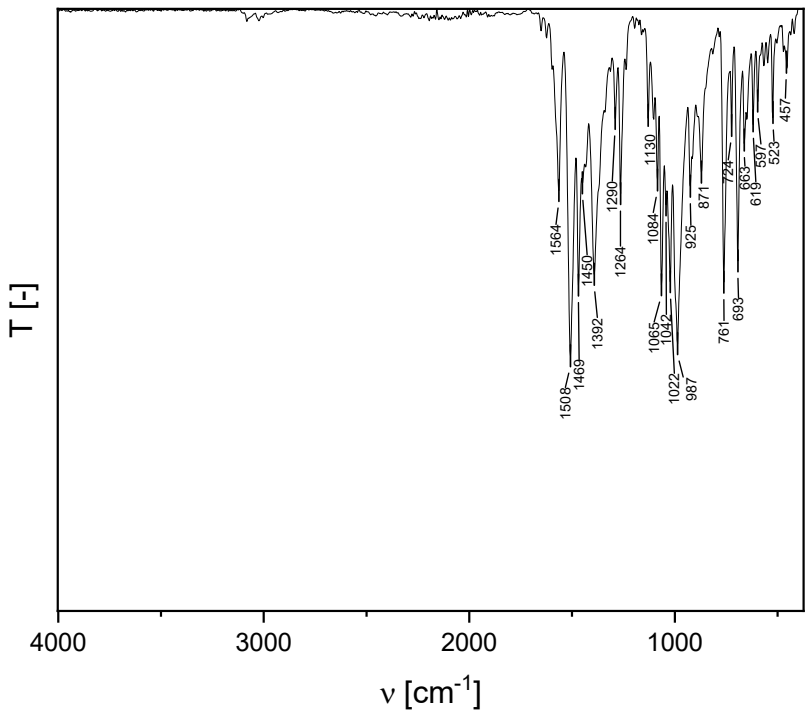

Fig. S44. ATR-IR spectrum of L'B($C_{14}H_{10}O_2$) (**13**).

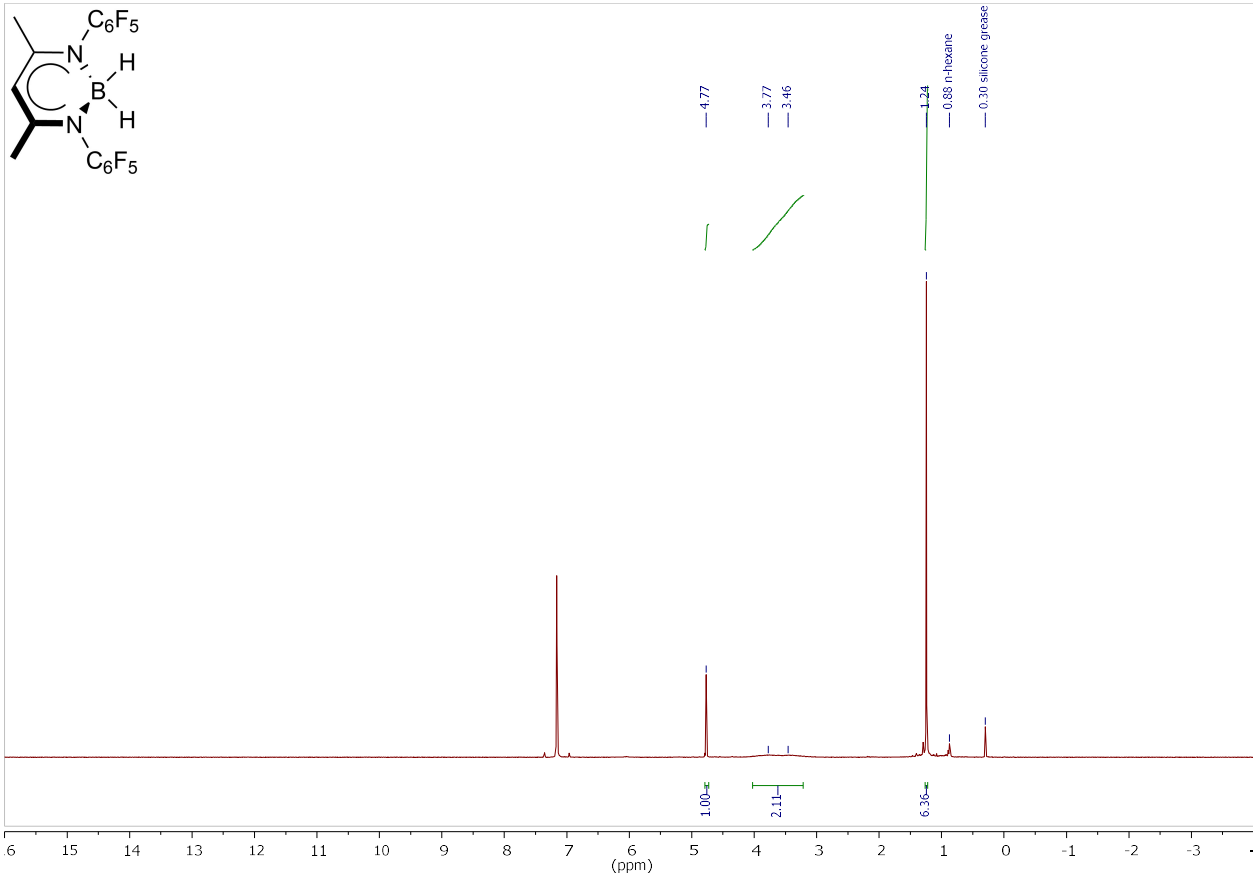

Fig. S45. ^{1}H NMR spectrum (400 MHz, C_6D_6, 25 °C) of L'BH_2 (**14**).

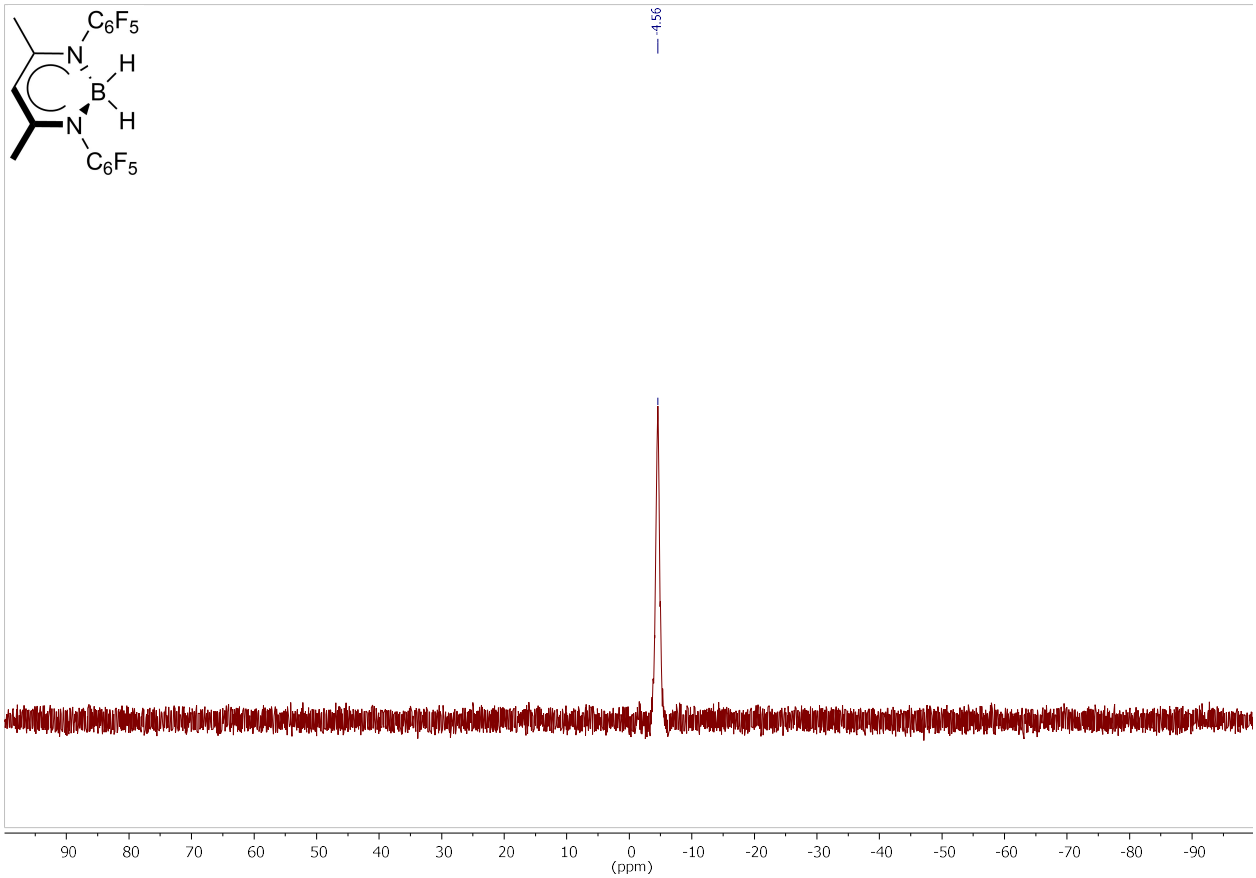

Fig. S46. ^{11}B NMR spectrum (192.5 MHz, C_6D_6, 25 °C) of L'BH_2 (**14**).

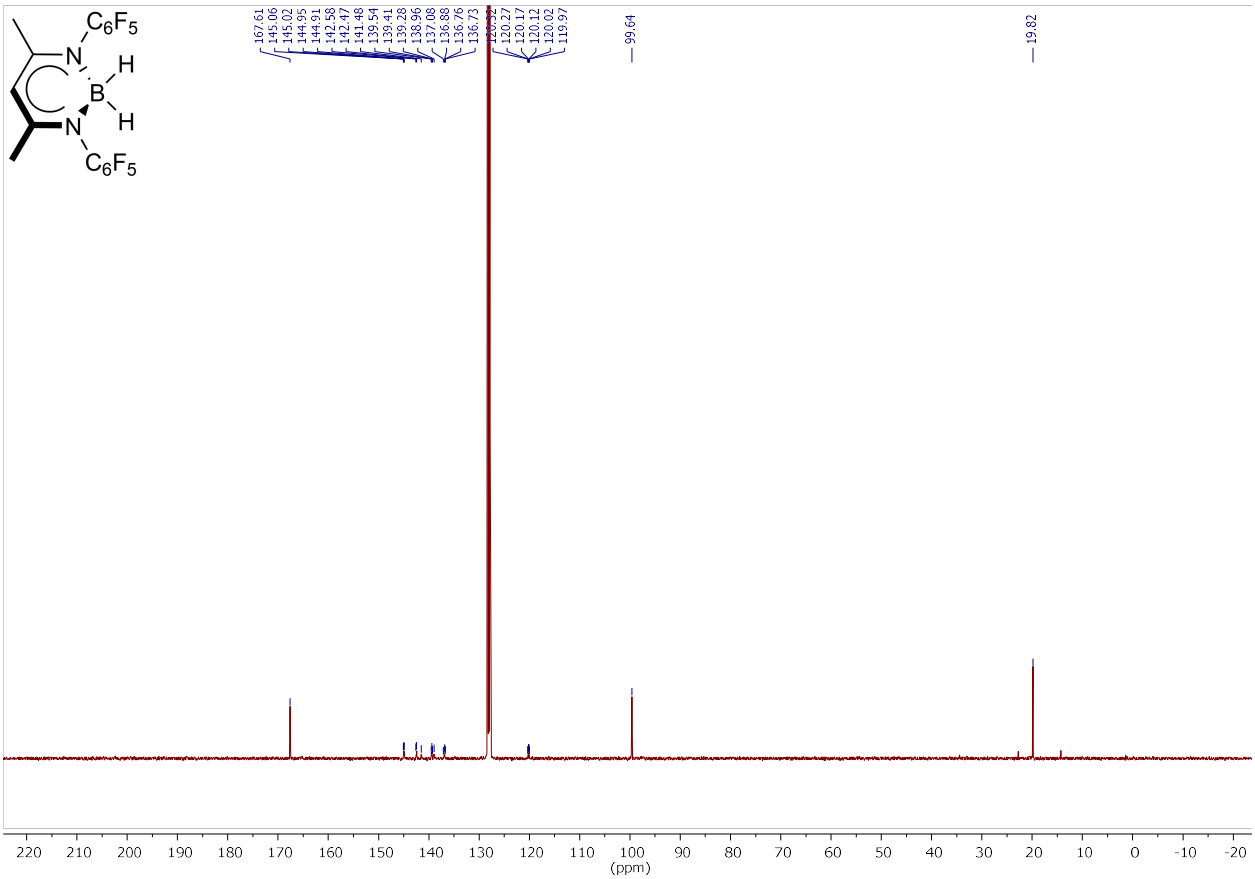

Fig. S47. ^{13}C NMR spectrum (100.6 MHz, C_6D_6, 25 °C) of L'BH_2 (**14**).

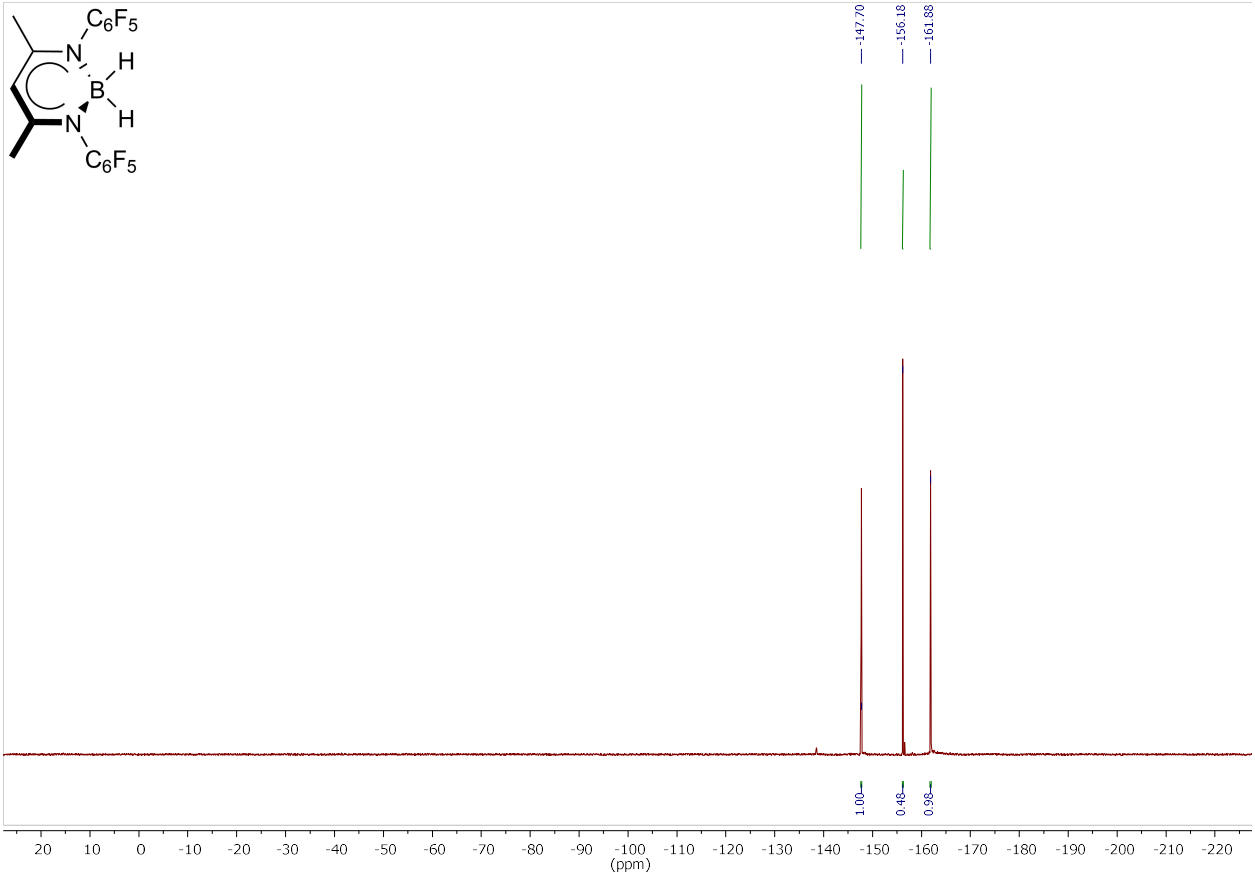

Fig. S48. ^{19}F NMR spectrum (376.5 MHz, C_6D_6, 25 °C) of L'BH_2 (**14**).

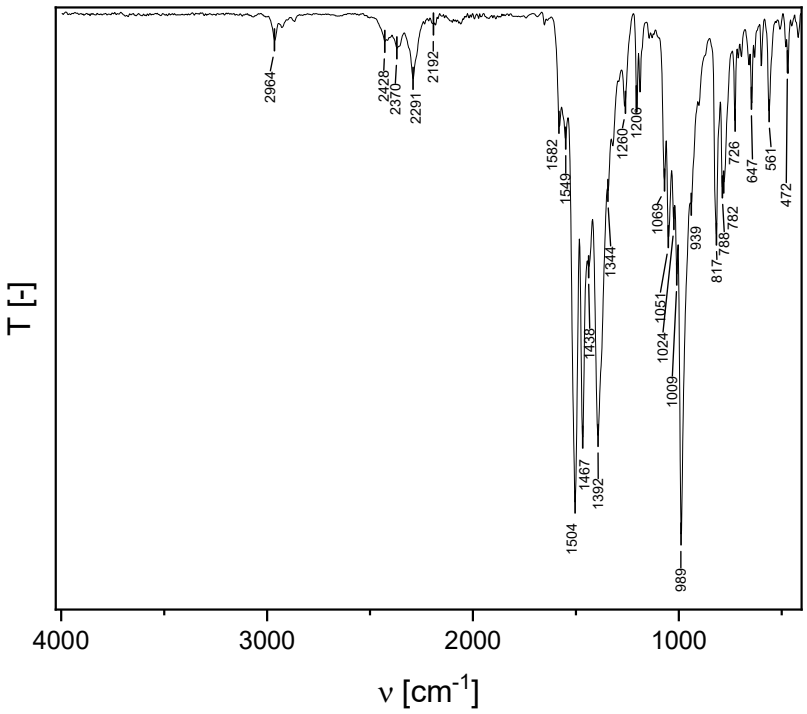

Fig. S49. ATR-IR spectrum of L'BH_2 (**14**).

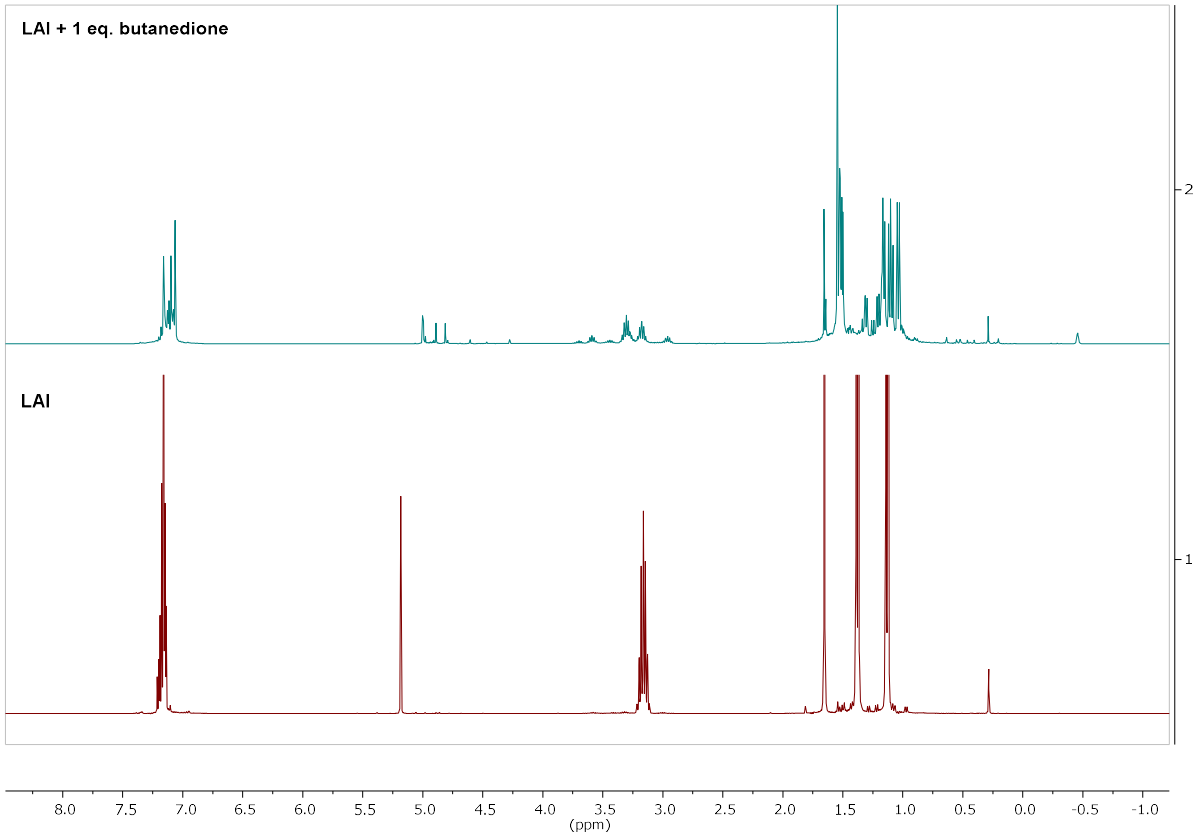

Fig. S50. Reaction of LAl with one equivalent of butanedione. Bottom: LAl before addition.

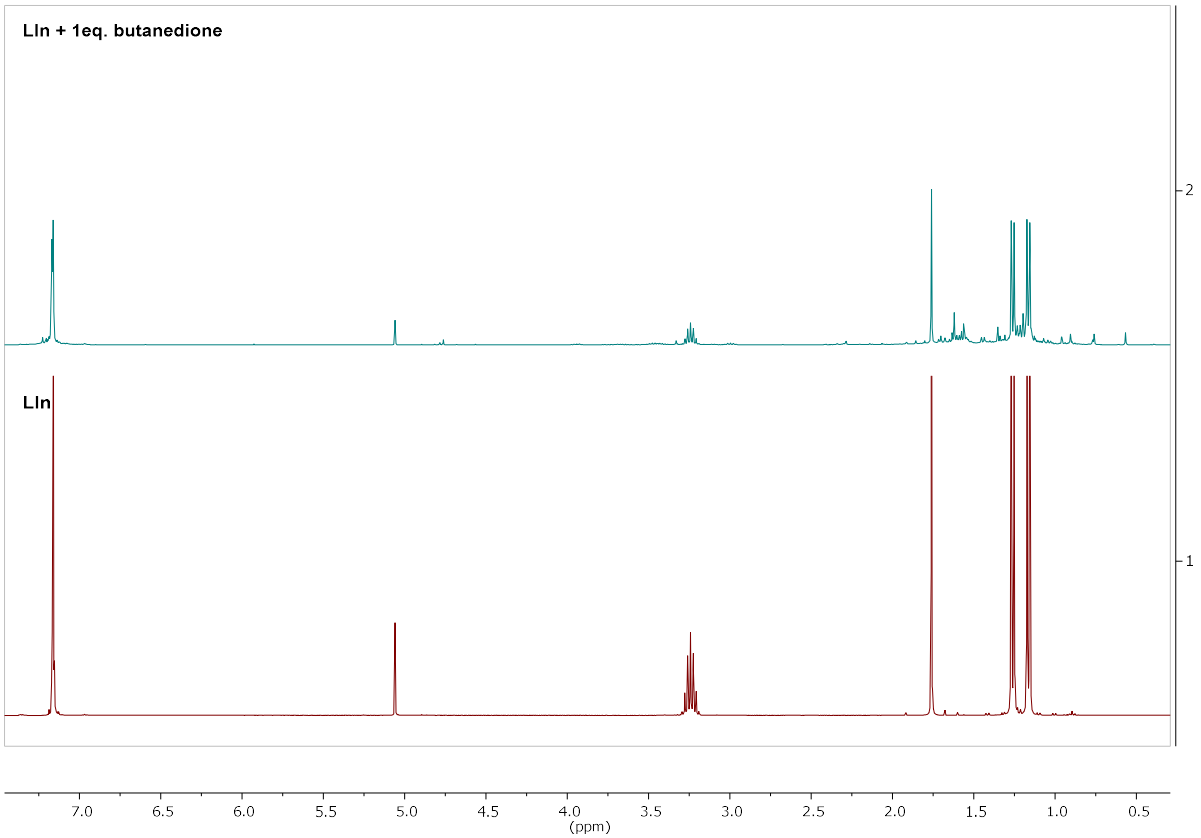

Fig. S51. Reaction of LIn with one equivalent of butanedione. Bottom: LIn before addition.

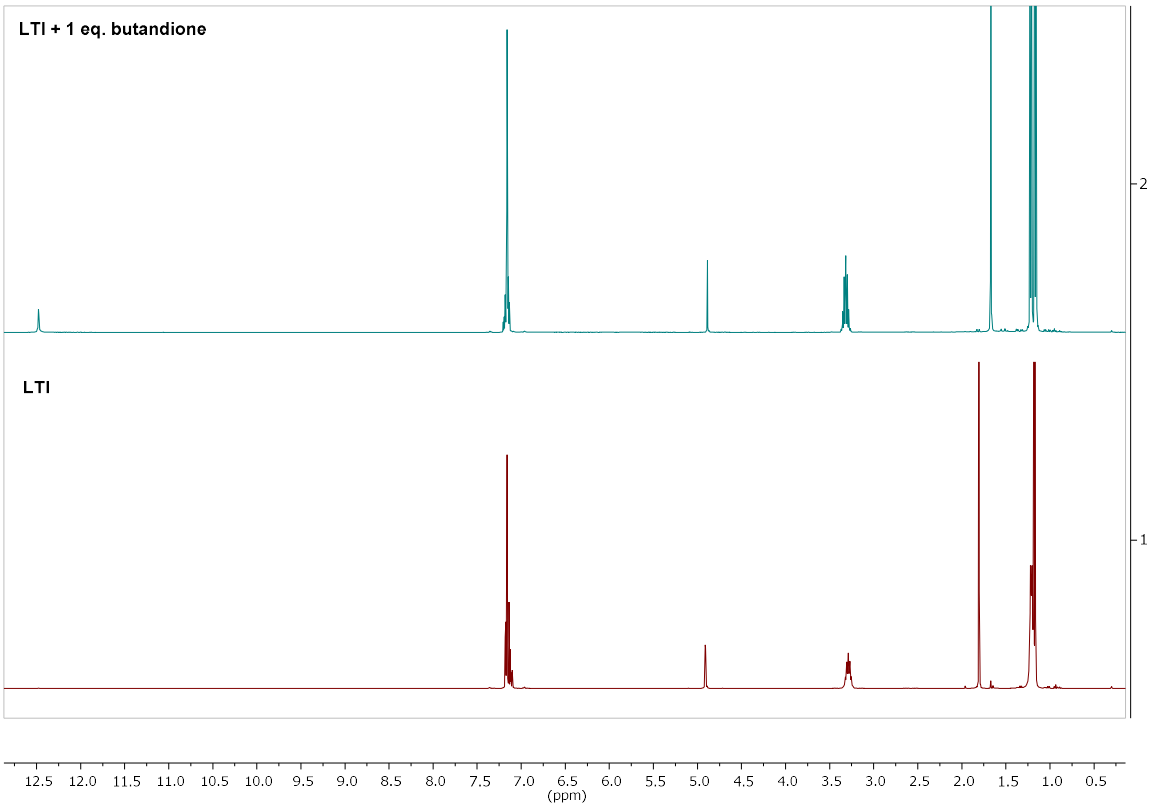

Fig. S52. Reaction of LTl with one equivalent of butanedione. Bottom: LTl before addition.

Table S1a. Crystallographic data of LGa($C_4H_6O_2$) (**1**), LGa($C_8H_{12}O_4$) (**2**), and LAl($C_{12}H_6O_2$) (**4**).

	1	**2**	**4**
Empirical formula	$C_{33}H_{47}GaN_2O_2$	$C_{43}H_{59}GaN_2O_4$	$C_{41}H_{47}AlN_2O_2$
M	573.44	737.64	626.78
Crystal size [mm]	0.277 × 0.175 × 0.073	0.371 × 0.240 × 0.192	0.258 × 0.115 × 0.114
T [K]	100(2)	100(2)	100(2)
Crystal system	monoclinic	orthorhombic	monoclinic
Space group	*C2/c*	$Pca2_1$	$P2_1/n$
a [Å]	20.0030(6)	22.8793(14)	12.9494(6)
b [Å]	19.8324(6)	17.9690(11)	20.0900(9)
c [Å]	17.6419(6)	19.4578(12)	13.6605(6)
α [°]	90	90	90
β [°]	115.0312(14)	90	97.216(2)
γ [°]	90	90	90
V [Å^3]	6341.3(4)	7999.5(9)	3525.7(3)
Z	8	8	4
D_{calc} [g·cm^{-3}]	1.201	1.225	1.181
μ(Mo/CuK$_\alpha$) [mm^{-1}]	1.406	0.730	0.782
Transmissions	0.75/0.57	0.75/0.67	0.75/0.66
F(000)	2448	3152	1344
Index ranges	$-25 \le h \le 25$	$-35 \le h \le 35$	$-16 \le h \le 15$
	$-25 \le k \le 25$	$-27 \le k \le 27$	$-25 \le k \le 25$
	$-22 \le l \le 22$	$-29 \le l \le 29$	$-17 \le l \le 17$
θ_{max} [°]	80.051	33.217	80.605
Refl. collected	130533	328650	147679
Independ. refl.	6890	30570	7713
R_{int}	0.1000	0.0539	0.0662
Refined parameters	376	1128	425
R_1 [I > 2σ(I)]	0.0297	0.0487	0.0358
wR_2 [all data]	0.0766	0.1290	0.0963
x(Flack)	–	0.398(12)	–
GooF	1.026	1.059	1.029
$\Delta\rho_{final}$ (max/min) [e·Å^{-3}]	0.403/-0.569	1.140/-0.527	0.241/-0.291

Table S1b. Crystallographic data of LGa($C_{12}H_6O_2$) (**5**), LIn($C_{12}H_6O_2$) (**6**), and LTl($C_{14}H_{10}O_2$) (**7**).

	5	**6**	**7**
Empirical formula	$C_{41}H_{47}GaN_2O_2$	$C_{87}H_{104}In_2N_4O_5$	$C_{94}H_{122}N_4O_4Tl_2$
M	669.52	1515.38	1780.69
Crystal size [mm]	0.386 × 0.349 × 0.174	0.186 × 0.151 × 0.081	0.204 × 0.072 × 0.034
T [K]	100(2)	100(2)	100(2)
Crystal system	monoclinic	monoclinic	triclinic
Space group	$P2_1/c$	$P2_1/n$	$P\bar{1}$
a [Å]	10.685(5)	13.2394(4)	12.4414(12)
b [Å]	20.803(10)	17.9680(6)	14.0266(13)
c [Å]	17.129(8)	16.9249(5)	14.6235(13)
α [°]	90	90	61.987(4)
β [°]	107.264(13)	92.4650(13)	74.874(5)
γ [°]	90	90	85.540(5)
V [Å^3]	3636(3)	4022.5(2)	2171.9(4)
Z	4	2	1
D_{calc} [g·cm^{-3}]	1.223	1.251	1.361
μ(Mo/CuK$_\alpha$) [mm^{-1}]	0.793	4.977	3.755
Transmissions	0.75/0.66	0.75/0.62	0.75/0.57
F(000)	1416	1584	908
Index ranges	$-16 \le h \le 15$	$-16 \le h \le 16$	$-16 \le h \le 16$
	$0 \le k \le 32$	$-22 \le k \le 22$	$-18 \le k \le 18$
	$0 \le l \le 26$	$-21 \le l \le 21$	$-19 \le l \le 19$
θ_{max} [°]	33.320	80.384	28.399
Refl. collected	182536	147879	99815
Independ. refl.	13884	8784	10869
R_{int}	0.1037	0.0604	0.0578
Refined parameters	425	425	460
R_1 [I > 2σ(I)]	0.0443	0.0198	0.0236
wR_2 [all data]	0.1349	0.0504	0.0574
GooF	1.048	1.029	1.037
$\Delta\rho_{final}$ (max/min) [e·Å^{-3}]	0.884/-0.709	0.438/-0.559	1.313/-1.115

Table S1c. Crystallographic data of $LAl(C_{14}H_{10}O_2)$ (**8**), $LGa(C_{14}H_{10}O_2)$ (**9**), $LIn(C_{14}H_{10}O_2)\cdot MeCN$ (**10**), and $LAl(C_{14}H_{10}O_2)_2$ (**11**).

	8	**9**	**10**	**11**
Empirical formula	$C_{43}H_{51}AlN_2O_2$	$C_{50.50}H_{58.50}GaN_2O_2$	$C_{45}H_{54}InN_3O_2$	$C_{142}H_{154}Al_2N_4O_8$
M	654.83	795.21	783.73	2098.64
Crystal size [mm]	0.435 × 0.210 × 0.070	0.154 × 0.117 × 0.051	0.257 × 0.229 × 0.110	0.216 × 0.184 × 0.160
T [K]	100(2)	100(2)	100(2)	100(2)
Crystal system	monoclinic	triclinic	orthorhombic	monoclinic
Space group	$P2_1/n$	$P\bar{1}$	$P2_12_12_1$	$P2_1/c$
a [Å]	22.055(11)	12.7707(9)	13.5750(8)	16.620(5)
b [Å]	17.741(9)	18.3465(8)	15.5145(9)	18.867(6)
c [Å]	22.328(12)	20.262(3)	19.4970(11)	19.008(6)
α [°]	90	100.364(5)	90	90
β [°]	118.486(8)	92.789(7)	90	99.398(5)
γ [°]	90	108.952(4)	90	90
V [Å^3]	7679(7)	4387.4(7)	4106.2(4)	5880(3)
Z	8	4	4	2
D_{calc} [g·cm^{-3}]	1.133	1.204	1.268	1.185
μ(Mo/CuK$_\alpha$) [mm^{-1}]	0.090	1.160	0.614	0.086
Transmissions	0.75/0.64	0.75/0.65	0.75/0.71	0.75/0.63
F(000)	2816	1690	1640	2248
Index ranges	$-29 \le h \le 29$	$-16 \le h \le 16$	$-22 \le h \le 22$	$-22 \le h \le 22$
	$-23 \le k \le 23$	$-23 \le k \le 23$	$-25 \le k \le 25$	$-25 \le k \le 25$
	$-29 \le l \le 29$	$-25 \le l \le 25$	$-32 \le l \le 32$	$-25 \le l \le 25$
θ_{max} [°]	28.758	80.731	36.386	28.368
Refl. collected	194136	260224	119647	133457
Independ. refl.	19336	19089	19997	14551
R_{int}	0.0993	0.0488	0.0293	0.0990
Refined parameters	885	1133	471	719
R_1 [I > 2σ(I)]	0.0477	0.0301	0.0210	0.0689
wR_2 [all data]	0.1258	0.0768	0.0512	0.1546
x(Flack)	–	–	-0.016(3)	–
GooF	1.017	1.043	1.049	1.126
$\Delta\rho_{final}$ (max/min) [e·Å^{-3}]	0.340/-0.364	0.315/-0.402	0.730/-0.334	0.866/-0.619

Table S1d. Crystallographic data of $(LAl)_2(C_{14}H_{10}O_2)$ (**12a,b**), and L'B$(C_{14}H_{10}O_2)$ (**13**).

	12a	**12b**	**13**
Empirical formula	$C_{84}H_{104}Al_2N_4O_2$	$C_{81}H_{113}Al_2N_4O_2$	$C_{31}H_{17}BF_{10}N_2O_2$
M	1255.67	1228.71	650.27
Crystal size [mm]	0.232 × 0.206 × 0.060	0.410 × 0.350 × 0.170	0.370 × 0.133 × 0.082
T [K]	100(2)	100(2)	100(2)
Crystal system	triclinic	triclinic	triclinic
Space group	$P\bar{1}$	$P\bar{1}$	$P\bar{1}$
a [Å]	12.3771(5)	12.902(2)	9.5575(5)
b [Å]	12.9748(5)	23.139(4)	9.9812(5)
c [Å]	24.5551(10)	25.361(4)	15.3139(7)
α [°]	97.796(2)	95.653(9)	98.5868(15)
β [°]	96.978(2)	104.445(8)	91.1274(14)
γ [°]	106.7538(19)	91.410(8)	106.0286(13)
V [Å^3]	3687.0(3)	7287(2)	1385.49(12)
Z	2	4	2
D_{calc} [g·cm^{-3}]	1.131	1.120	1.559
μ(Mo/CuK$_\alpha$) [mm^{-1}]	0.725	0.088	1.266
Transmissions	0.75/0.68	0.75/0.68	0.75/0.64
F(000)	1356	2676	656
Index ranges	$-15 \le h \le 15$	$-18 \le h \le 18$	$-11 \le h \le 12$
	$-16 \le k \le 16$	$-33 \le k \le 33$	$-12 \le k \le 12$
	$-31 \le l \le 31$	$-36 \le l \le 36$	$-19 \le l \le 19$
θ_{max} [°]	80.424	30.508	80.165
Refl. collected	213903	250130	76757
Independ. refl.	15992	44487	6000
R_{int}	0.0631	0.0834	0.0290
Refined parameters	904	1677	417
R_1 [I > 2σ(I)]	0.0342	0.0531	0.0310
wR_2 [all data]	0.0889	0.1385	0.0824
GooF	1.028	1.006	1.040
$\Delta\rho_{final}$ (max/min) [e·Å^{-3}]	0.277/-0.280	0.629/-0.536	0.258/-0.233

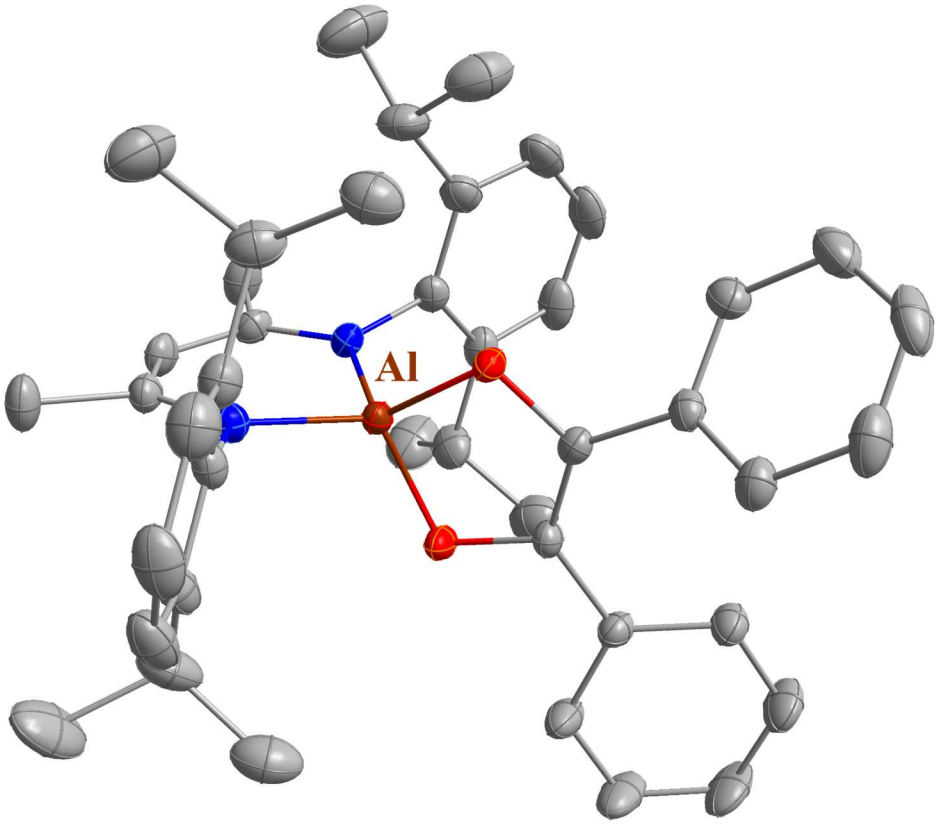

Fig. S53. Molecular structure of one of the two independent molecules of LAl($C_{14}H_{10}O_2$) (**8**) in its crystals. Displacement ellipsoids are drawn at the 50% probability level and H atoms are omitted.

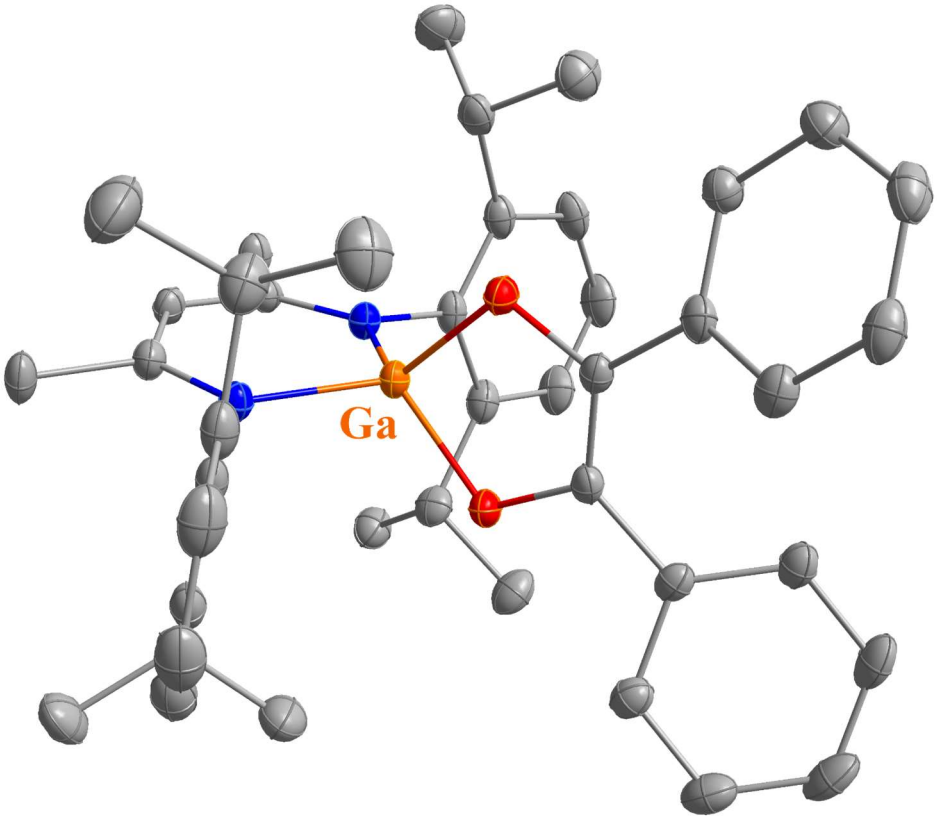

Fig. S54. Molecular structure of one of the two independent molecules of LGa($C_{14}H_{10}O_2$) (**9**) in its crystals. Displacement ellipsoids are drawn at the 50% probability level. Only the major component of disorders is shown, and H atoms are omitted.

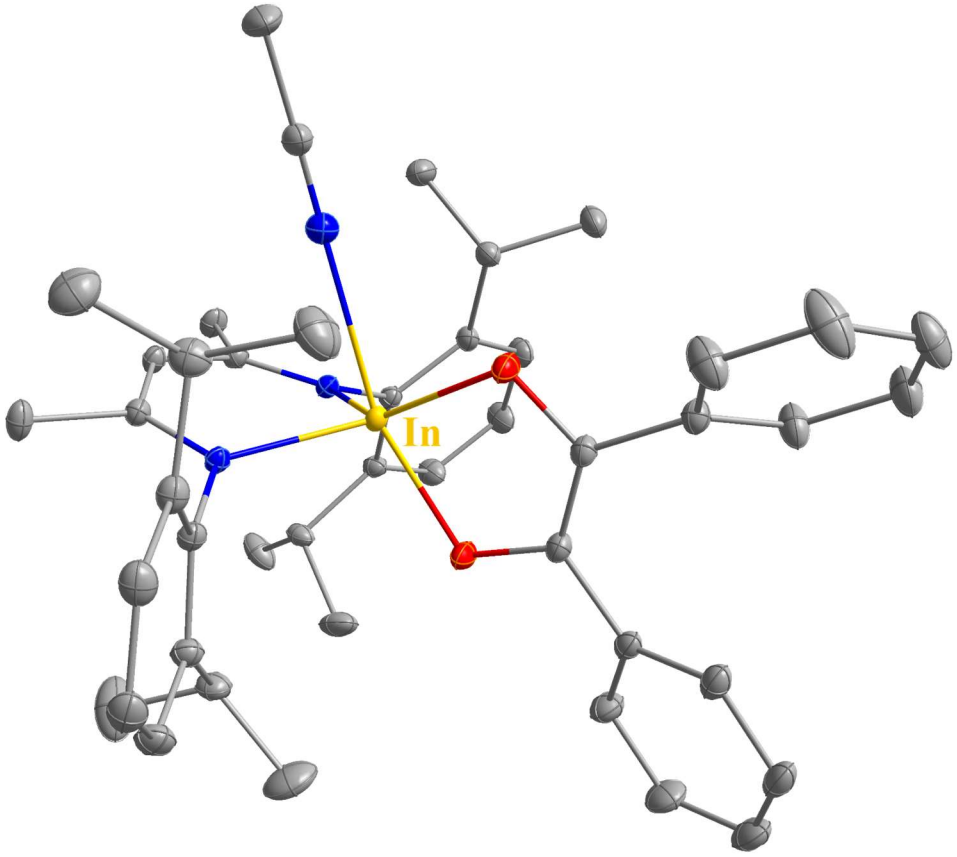

Fig. S55. Molecular structure of $LIn(C_{14}H_{10}O_2)\cdot MeCN$ (**10**) in its crystals. Displacement ellipsoids are drawn at the 50% probability level.

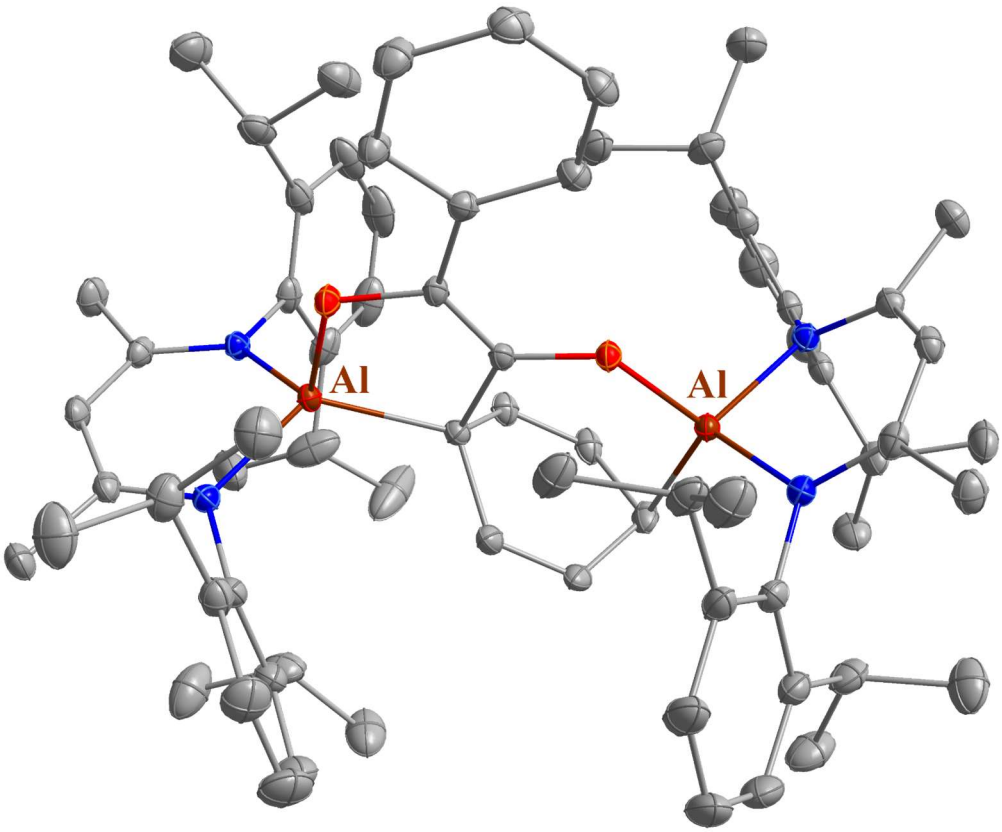

Fig. S56. Molecular structure of one of the two independent molecules of $(LAl)_2(C_{14}H_{10}O_2)$ (**12b**) in its crystals. Displacement ellipsoids are drawn at the 50% probability level, and H atoms are omitted.

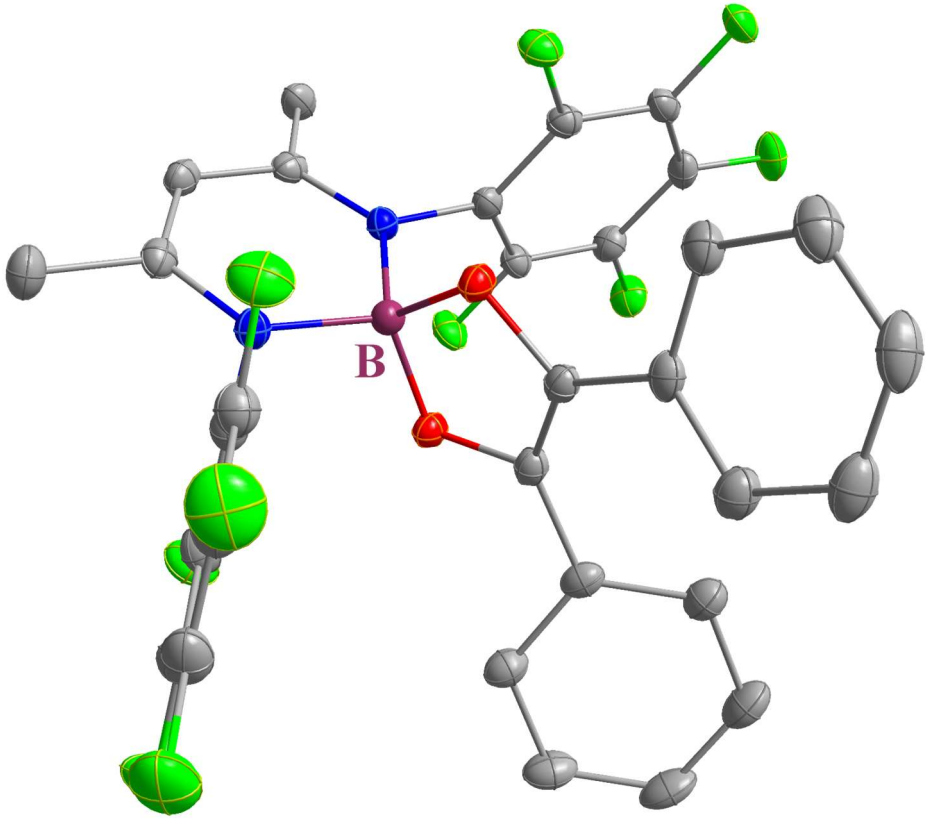

Fig. S57. Molecular structure of one of the two independent molecules of L'B($C_{14}H_{10}O_2$) (**13**) in its crystals. Displacement ellipsoids are drawn at the 50% probability level, and H atoms are omitted.